Modeling the Continuous and Jump Dynamics of Stock Movements Using Price Range

Chen-Sheng Lin[†] **Ray Yeutien Chou**[‡]

This version: July 2021

ABSTRACT

This study presents new evidence on the role of volatility jumps under the range-based model. We dissect the components of the high–low range into its continuous and discontinuous (jump) parts, using daily realized measures data from the Oxford–Man Realized Library. Based on the conditional autoregressive range (CARR) model, a new model called CARR-CJ is developed by separately modeling the dynamics of the continuous variation and jumps in the range. The results reveal that the jump component has longer volatility half-life and smaller short-run impact on future volatility compared to the continuous component, an indication of the differences in the dynamics of the two range processes. More importantly, the CARR-CJ model performs significantly better than the CARR benchmark as well as the heterogeneous autoregressive with continuous volatility and jumps (HAR-CJ) model for both in-sample fit and out-of-sample forecasting, especially at longer forecast horizons. Moreover, the results of this study are quite robust to employ other volatility measures and forecast evaluation methods, as well as include well-known exogenous variables, such as the leverage effect, into the CARR-CJ model.

Keywords: Volatility forecasting; Jumps; Price range; CARR-CJ; CARR
JEL classification: C22, C51, C53

[†] The Research Institute for the Humanities and Social Sciences, Ministry of Science and Technology. E-mail: imfdavidlin@gmail.com.
[‡] Institute of Economics, Academia Sinica. E-mail: rchou@econ.sinica.edu.tw.

1. INTRODUCTION

As the seminal paper by Merton (1976) considered jumps in asset prices when analyzing movements in markets, a growing number of studies have started to address the issue of detecting jumps and measuring the sizes thereof (Andersen et al., 2007; Christensen et al., 2010; Corsi et al. 2010, among others). Aït-Sahalia (2004) indicated that jumps play an important role in finance, such as in risk management, portfolio allocation, and derivative pricing.

In theory, at present, there are two primary procedures to test the presence of jumps, namely, parametric and nonparametric. The parametric procedure relies on low-frequency transaction data (Aït-Sahalia, 2002; Andersen et al., 2002; Eraker et al., 2003), while the nonparametric procedure exploits high-frequency transaction prices or mid-quotes in a model free framework (Andersen et al., 2007; Andersen et al., 2009; Corsi et al., 2010; Jiang and Oomen, 2008; Lee and Mykland, 2008; Mancini, 2009; Podolskij and Ziggel, 2010). Barndorff-Nielsen and Shephard (2004, 2006) were pioneers in the use of five-minute high-frequency data for constructing the so-called bipower variation and nonparametrically separate the quadratic variation process into its continuous and jump components. Building on their theoretical method, Andersen et al. (2007) and Corsi et al. (2010) decomposed the realized volatility into its continuous and discontinuous jump parts and established a heterogeneous autoregressive with continuous volatility and jumps (HAR-CJ) model, which provided superior predictability of future volatility. Corsi and Renó (2012) further proposed a LHAR-CJ model based on the HAR-CJ model with leverage effects and suggested that the continuous variation and jump component had different dynamics, and thus, should be modeled separately; neglecting each one of them is detrimental to the forecasting performance. In another study by Buncic and Gisler (2017), they evaluated the importance of jumps and the leverage effect on the high-frequency realized volatility in eighteen international equity markets, using the HAR-CJ and LHAR-CJ models. They found that the separation of realized volatility into a continuous and a jump component is beneficial only for the S&P 500 index and it has limited value for the non-US markets. It is noteworthy that results from the abovementioned studies are almost exclusively grounded upon the return-based volatility models, while completely ignoring the application of range-based volatility models in finance.

It is a well-known fact that high–low range is considered as an alternative to measuring, modeling, and forecasting asset volatility. Parkinson (1980) stated that the range is an effective estimator of volatility regardless of any interval. Empirical results of Brandt and Jones (2006) and Molnár (2016) determined that using the price range to proxy volatility in the generalized autoregressive conditionally heteroscedastic (GARCH) type models produced better out-of-sample forecasting performance. Degiannakis and Livada (2013) also show, using simulation studies, that the range as a volatility estimator is more accurate than the realized volatility estimator. Chou (2005) first proposed a range-based conditional autoregressive range (CARR) model to describe the dynamics of the price range and found that the CARR model significantly outperformed the renowned GARCH model.[1] Nevertheless, a few studies have focused on the role

[1] For a comprehensive review of the important developments in ways of estimating range-based volatility, see Chou

of jumps in price range. For example, Christensen and Podolskij (2006) were pioneers to propose the significant jump test in the framework of the realized range-based volatility (RRV). In empirical work, Caporin et al. (2015) and Ma et al. (2018) investigated the contribution of jumps on forecasts of the daily RRV based on the HAR-type specifications.

Contrary to realized measures models, this paper aims to consider the importance of jumps in volatility forecasting by directly using the range-based model. For this purpose, we introduce a CARR-CJ model with jumps as an alternative approach, which extends the original CARR model by modeling the continuous and discontinuous (jump) parts of a range separately. The motivation for using the price range instead of the high-frequency data based realized range is that the realized range is not often publicly available, but the low-frequency data based price range is usually free and widely available. Following Andersen et al. (2007), we utilize aggregate daily realized measures data from the Oxford–Man Realized Library and nonparametrically separate the daily price range into its continuous and jump components. To the best of our knowledge, the present study is the first to incorporate jumps in a low-frequency price range modeling and forecasting based on the classic CARR framework.

Various international equity market indices are examined comprehensively to evaluate the relative performance of the CARR-CJ model against the CARR benchmark and the HAR-CJ model of Andersen et al. (2007). Empirical evidence shows that the jump component has longer volatility half-life and smaller short-run impact on future volatility than the continuous component; an indication that the market dynamics for the continuous and jump parts of a range are very different. In this paper, each component was modeled via a separate CARR model with its own parameters. Moreover, the CARR-CJ model outperforms the CARR benchmark as well as the HAR-CJ model for in-sample fit and out-of-sample forecasting. We note that the improvements in forecast performance are particularly apparent for longer forecast horizons. In addition, our results have been found to be quite robust to employ other volatility measures and forecast evaluation methods, as well as include well-known exogenous variables, such as the leverage effect, into the CARR-CJ model.

Our paper makes several contributions. First, existing studies on the role of jumps in financial markets are almost exclusively grounded upon HAR framework using realized measures. To fill this gap, we are the first to propose a new range-based model with jumps dubbed CARR-CJ, which should enrich the related research on volatility jumps. Moreover, the Oxford–Man Realized Library database is publicly available and contains aggregate daily realized measures; thus, access to the high-frequency intraday data from which these realized measures were constructed is not required. Second, based on a non-linear dynamic structure, our model is different from the HAR-type models, that are built on a simple linear regression structure. That is, the proposed model has more flexibility to capture the dynamic behavior of volatilities. Thus, we can analyze the asymmetry of the continuous and jump parts of a range by comparing the magnitudes of the short-run impact and long-run persistence in nature. Empirical results provide consistent evidence

et al. (2015).

supporting the asymmetry between these two parts. Third, by decomposing price range into jumps and continuous variation, our model can yield substantial improvements in volatility forecasting compared with the CARR and HAR-CJ models, especially at longer horizon forecasts. It is clear from this study that each of the components in the price range plays an unneglectable role in explaining future volatility based on the framework of the range-based model, mainly because jumps not only convey additional trading information but also remove noise from the continuous component (Corsi et al., 2010). These findings can be of great importance for some relevant financial applications, such as risk management and asset pricing.

The rest of the paper is organized as follows. Section 2 presents a brief review of the classic CARR model and proposes the CARR-CJ model with theoretical discussions. Section 3 outlines the econometric methodologies used in this paper. Section 4 describes the detailed empirical results. Section 5 contains some concluding remarks.

2. THE CARR-CJ MODEL

Let p_t denote a logarithmic asset price at time *t*, driven by a geometric Brownian motion with stochastic volatilities. We let p_t^H and p_t^L be the high and low prices in natural logarithm on day *t*. Hence, the logarithmic price range R_t can be defined as follows:

$$R_t = p_t^H - p_t^L . \tag{1}$$

Garman and Klass (1980) reported that the price range is a highly efficient volatility estimator compared with the return-based estimator.

One of the first range-based models to capture the time variation of volatility (Chou, 2005) was the CARR model, which is now most commonly used as a benchmark range model. The CARR(*p*,*q*) has the following form:

$$R_t = \lambda_t \varepsilon_t ,$$

$$\lambda_t = \omega + \sum_{i=1}^{p} \alpha_i R_{t-i} + \sum_{j=1}^{q} \beta_j \lambda_{t-j} ,$$

$$\varepsilon_t | I_{t-1} \sim f(1, \cdot), \text{ i.i.d.} ,$$

$$1 > \sum_{i=1}^{p} \alpha_i + \sum_{j=1}^{q} \beta_j , \alpha_i > 0, \beta_j > 0 ,$$

where $\lambda_t \equiv E[R_t | I_{t-1}]$ represents the conditional mean of the range based on all information up to day *t*−1. The parameters ω, α_i, and β_j characterize the inherent uncertainty in the range, the short-term impact, and the long-term effect of shocks to the range, respectively. Generally, coefficient α_i tells us how much weight we assign to the most recently observed volatility proxy (price ranges). If we receive a larger α_i, the performance of the model should be better. The distribution of the disturbance term ε_t, or the so-called normalized range $\varepsilon_t = R_t / \lambda_t$, is assumed to be dispersed with a nonnegative density function $f(\cdot)$ with a unit mean. Chou (2005) empirically

demonstrated that the CARR model dominated the GARCH model in forecasting volatilities of S&P 500 using daily and weekly observations. Since it is generally known that CARR(p,q) of an order higher than (1,1) is seldom useful (see, e.g., Chou, 2005; Chou and Liu, 2010; Xie, 2019), we study the CARR model only in its simplest version, i.e., the CARR(1,1) model:

$$\lambda_t = \omega + \alpha R_{t-1} + \beta \lambda_{t-1}. \tag{2}$$

Since we do not study CARR models of higher orders, we sometimes refer to the CARR(1,1) model simply as the CARR model.

We proceed to demonstrate how to identify the continuous and jump parts of a range while constructing the CARR-CJ model. In financial econometrics, it is well known that the quadratic variation (QV) that measures the variation of asset price processes is composed of a continuous and a discontinuous (or jump) part, defined as follows:

$$QV_t = \int_{t-1}^{t} \sigma_s^2 ds + \sum_{t-1<s\le t} \kappa_s^2 , \tag{3}$$

where $\int_{t-1}^{t} \sigma_s^2 ds$ is the continuous integrated variation of the process, and κ_s^2 is the squared discontinuous jump at time s. Inference on the continuous and jump parts of QV_t has been studied in detail in the literature (see, e.g., return-based theory of Andersen et al., 2007 and range-based theory of Christensen and Podolskij, 2006, 2007). Given the asymptotic theory, these two methodologies can draw the same inferences about the diffusive and jump components. Due to the availability of realized return-based measures, we resort to employ the return-based theory for making inferences. We start by introducing the notational framework.[2]

The empirical counter part of QV_t is called the realized variance (RV), which is simply the sum of squared observed intraday returns,

$$RV_t = \sum_{i=1}^{M} r_{t,i}^2 , \tag{4}$$

where $r_{t,i} = p_{t,i} - p_{t,i-1}$ denotes the time t log return observed in the i-th interval of an equidistant grid on $[t-1, t]$, with a total of M intervals and $M + 1$ observed log-prices $p_{t,i}$. It is well known that RV_t is a consistent estimator for QV_t,

$$RV_t \xrightarrow{p} QV_t . \tag{5}$$

However, in the presence of jumps, RV_t is biased for the integrated variation with the jump terms inducing the bias. Alternatively, the (realized) bipower variation (BPV) of Barndorff-Nielsen and Shephard (2004), defined as the sum of the product of adjacent absolute intraday log returns standardized by a constant, is a consistent estimator for the continuous variation even in the presence of jumps:

[2] Note here that since we are working with a publicly available database that contains aggregate daily realized return-based measures and we do not have access to the high-frequency intraday data from which these were constructed, it is not feasible for us to employ the range-based theory.

$$BPV_t = \mu^{-2} \sum_{i=2}^{M} |r_{t,i}||r_{t,i-1}| \xrightarrow{M\to\infty} \int_{t-1}^{t} \sigma_s^2 ds\,, \tag{6}$$

where $\mu = \sqrt{2/\pi} \approx 0.79788$ is a finite sample bias correction term , M is the sample frequency within interval $[t-1, t]$, and $r_{t,i}$ is the discretely-sampled i-th intraday log return for day t. Thus, the difference between RV_t and BPV_t consistently estimates the part of QV_t due to jumps as:

$$J_t = RV_t - BPV_t \xrightarrow{M\to\infty} \sum_{t-1<s\le t} \kappa_s^2\,. \tag{7}$$

To prevent the estimates of the squared jump variation defined by the right hand-side of Eq. (3) from being negative in finite samples, we follow Barndorff-Nielsen and Shephard (2004) to truncate the actual empirical measurements at zero. That is:

$$J_t = \max[RV_t - BPV_t, 0]\,. \tag{8}$$

The continuous component then is defined as:

$$C_t = RV_t - J_t \xrightarrow{M\to\infty} \int_{t-1}^{t} \sigma_s^2 ds\,. \tag{9}$$

These estimators provide a complete decomposition of QV_t. Following Aït-Sahalia and Jacod (2012), we denote the relative contribution of continuous variation and jumps, respectively, to QV_t as follows:

$$\theta_t^C = \frac{C_t}{QV_t}\,, \tag{10}$$

$$\theta_t^J = \frac{J_t}{QV_t}\,, \tag{11}$$

where $\theta_t^C + \theta_t^J = 1$. Christensen and Podolskij (2006) proposed a range-based theory to replace RV with the squared range to draw inference about QV_t of asset prices. According to their work, the partitioning of squared range induced by the continuous and jump components can be done using their respective contribution to QV_t, that is:

$$\begin{aligned} R_t^2 &= \underbrace{\theta_t^C R_t^2}_{\text{continuous part}} + \underbrace{\theta_t^J R_t^2}_{\text{jump part}} \\ &= \left(\sqrt{\theta_t^C}\, R_t\right)^2 + \left(\sqrt{\theta_t^J}\, R_t\right)^2 \\ &= \left(CR_t\right)^2 + \left(JR_t\right)^2, \end{aligned} \tag{12}$$

where CR_t and JR_t denote the continuous and the jump part of a price range, respectively. In other words, CR_t is estimated by $\sqrt{\theta_t^C}\, R_t$ and JR_t is estimated by $\sqrt{\theta_t^J}\, R_t$. We will use this decomposition of price range extensively in our analysis below.

Grounded on the above, we can establish a CARR-CJ model to make empirical researches on both CR_t and JR_t in a range volatility to forecast the future volatility in financial markets. The CARR-CJ model of order (p,q) is presented as follows:

$$R_t = \sqrt{CR_t^2 + JR_t^2}\,,$$

$$CR_t = \lambda_t^C \varepsilon_t^C\,,$$

$$JR_t = \lambda_t^J \varepsilon_t^J\,,$$

$$\lambda_t^C = \omega^C + \sum_{i=1}^{p} \alpha_i^C CR_{t-i} + \sum_{j=1}^{q} \beta_j^C \lambda_{t-j}^C\,,$$

$$\lambda_t^J = \omega^J + \sum_{i=1}^{p} \alpha_i^J JR_{t-i} + \sum_{j=1}^{q} \beta_j^J \lambda_{t-j}^J\,,$$

$$\varepsilon_t^C \big| I_{t-1} \sim f^C(1,\cdot), \text{i.i.d.}\,,$$

$$\varepsilon_t^J \big| I_{t-1} \sim f^J(1,\cdot), \text{i.i.d.}\,,$$

$$1 > \sum_{i=1}^{p} \alpha_i^C + \sum_{j=1}^{q} \beta_j^C, \alpha_i^C > 0, \beta_j^C > 0\,,$$

$$1 > \sum_{i=1}^{p} \alpha_i^J + \sum_{j=1}^{q} \beta_j^J, \alpha_i^J > 0, \beta_j^J > 0\,.$$

Under this approach, the different dynamics of the continuous and jump components can be characterized by the different values of pairs of parameters, (ω^C, ω^J), (α_i^C, α_i^J), and (β_j^C, β_j^J), and the disturbance density $(f^C(1,\cdot), f^J(1,\cdot))$. Empirical studies on five major international equity market indices (Australia AORD, American DJI and S&P 500, Hong Kong HSI, and Japan NK 225) have demonstrated that the market dynamics of these two range processes are indeed different and that the CARR-CJ model can outperform the standard CARR model in volatility forecasting. Furthermore, to evaluate the superiority of the CARR-CJ model, we also study its simplest version, i.e., the CARR-CJ(1,1) model:

$$\lambda_t^C = \omega^C + \alpha^C CR_{t-1} + \beta^C \lambda_{t-1}^C\,, \tag{13}$$

$$\lambda_t^J = \omega^J + \alpha^J JR_{t-1} + \beta^J \lambda_{t-1}^J\,. \tag{14}$$

3. MODEL ESTIMATION AND FORECAST

Given that the CARR-CJ model has exactly the same form as the CARR model, the two models in our paper are estimated consistently via quasi-maximum likelihood estimation (QMLE) method.[3] Since the evolutions of the continuous and jump parts are specified independently, the two parts can be estimated separately. Specifically, assuming that the disturbance term follows an exponential distribution with unit mean and using R_t as a general notation of CR_t and JR_t, the log-likelihood function for each part of the range series can be written as follows:[4]

[3] Engle and Russel (1998) proved that under some regularity conditions, parameters in the CARR models can be estimated consistently by QMLE in which the density function of the disturbance term ε_t is given by a unit mean exponential density function. See also Engle (2002) for further discussions.

[4] Chou (2005) substantiated that the exponential density function can be used for constructing the likelihood to

$$LLF = -\sum_{t=1}^{T}\left[\ln(\lambda_t) + \frac{R_t}{\lambda_t}\right], \tag{15}$$

where T is the sample size.

Both in-sample and out-of-sample forecasts are used to assess the performance of the CARR and CARR-CJ models. We start by comparing the in-sample forecasting power of these two volatility models by calculating the mean absolute error (MAE), the root mean squared error (RMSE), and the quasi-likelihood (QLIKE) of Bollerslev et al. (1994) as follows:

$$\mathrm{MAE}(m) = T^{-1}\sum_{t=1}^{T}\left|\mathrm{MV}_t - \mathrm{FV}_t(m)\right|, \tag{16}$$

$$\mathrm{RMSE}(m) = \left[T^{-1}\sum_{t=1}^{T}\left(\mathrm{MV}_t - \mathrm{FV}_t(m)\right)^2\right]^{0.5}, \tag{17}$$

$$\mathrm{QLIKE}(m) = T^{-1}\sum_{t=1}^{T}\left(\frac{\mathrm{MV}_t}{\mathrm{FV}_t(m)} - \ln(\frac{\mathrm{MV}_t}{\mathrm{FV}_t(m)}) - 1\right), \tag{18}$$

where MV_t and $\mathrm{FV}_t(m)$ are the measure of volatility and the forecasted value reported by model m, respectively. Smaller MAE, RMSE, and QLIKE represent lower forecasting error. According to Patton (2011), the QLIKE statistic is more consistent and robust to outliers in volatility proxy than others, indicating that the error emanated from using a noisy proxy does not change the ranking of our forecasting methods.

To examine the differences between the forecasting powers of these two competing volatility models, CARR and CARR-CJ, we follow Mincer and Zarnowitz (1969) and run the following regression:

$$\mathrm{MV}_t = a + b\mathrm{FV}_t(m) + u_t. \tag{19}$$

For the CARR-CJ model, the range forecasts are obtained by taking the sum of the forecasts of the continuous and jump parts. A test of the unbiasedness of the predicted volatility can be performed by a joint test of $a = 0$ and $b = 1$. Adjusted R-squared value is also used as the criterion for assessing forecasting powers of different models.[5] Since volatility is a latent variable, we use the 5-min realized volatility as the measure of volatility, defined as follows:

$$\sigma_{RV} = \sqrt{\sum_{i=1}^{M} r_{t,i}^2}, \tag{20}$$

where $r_{t,i}$ denotes the time t log return observed in the i-th interval of an equidistant grid.

To determine the relative information content of the two competing volatility models, we also run a forecast encompassing regression developed by Chong and Hendry (1986) from Eq. (19):

$$\mathrm{MV}_t = a + b\mathrm{FV}_t(\mathrm{CARR}) + c\mathrm{FV}_t(\mathrm{CARR\text{-}CJ}) + u_t. \tag{21}$$

consistently estimate the parameters by QMLE in the conditional mean equation.

[5] Note here that the range forecasts through CARR-type models usually have a scale difference from the measured volatilities (e.g., return-based volatility), so FV_t will not have a coefficient of unity even if it is unbiased. Following Chou (2005), we therefore focus primarily on the comparison of forecast powers of the two competing models.

The model positioned in front and behind of the encompassing regression refers to a benchmark and the competing model, respectively. The null hypothesis is that the benchmark model encompasses the competing model. When $b = 0$ and $c \neq 0$, the null hypothesis should be rejected, and we conclude that the competing model contains information that the benchmark model does not. Similarly, we say that the benchmark model encompasses the competing model if $b \neq 0$ and $c = 0$. When both parameters have non-zero values (i.e., *b* and *c* are both significantly different from zero), then the competing model is believed to cover information that is in addition to that delivered by the benchmark model.

For out-of-sample forecasts, we analyze the one- and multi-step-ahead forecasts because it is useful to compare these two models at longer horizons, and following Chou (2005), a rolling (moving) window estimation procedure is carried out. For multi-step-ahead predictions, the iterated strategy is implemented in our study. To be specific, the whole *T* data observations are divided into an in-sample portion composed of the first *k* observations and an out-of-sample portion composed of the last *s* observations. An initial sample using observations 1 to *k* is used to estimate the models and to form *h*-step ahead out-of-sample forecasts starting at time *k*. Then the window is moved ahead one-time period, the models are re-estimated using observations 2 to *k* + 1 and *h*-step ahead out-of-sample forecasts are produced starting at time *k* + 1. This process is repeated until all forecasts for the out-of-sample period are obtained.

Brandt and Jones (2006) argued that these forecast evaluation statistics were not capable of testing whether the difference between forecasting performances is significant from the statistical view. To tackle this problem, we employ the Diebold and Mariano (1995) (henceforth DM) to test the null hypothesis that the two forecast series have exactly the same predictive accuracy and hence are statistically indistinguishable. Let the forecast error of model *i* be

$$e_{i,t} = \mathrm{MV}_t - \mathrm{FV}_{i,t}. \tag{22}$$

We test the superiority of model *i* over model *j* with a *t*-test of $\mu_{i,j}$ coefficient with heteroskedasticity and autocorrelation consistent (HAC) robust standard errors because loss differentials may be serially correlated as follows:

$$e_{i,t}^2 - e_{j,t}^2 = \mu_{i,j} + \eta_t, \tag{23}$$

where a negative estimate of $\mu_{i,j}$ indicates support for model *i* and η_t is an *i.i.d.* zero-mean error term. We set the newly proposed CARR-CJ model as model *i*, and the standard CARR model as model *j* in this paper.

It should be underlined that the values forecasted through the CARR and CARR-CJ models usually have a scale difference from MV (see Parkinson, 1980).[6] Thus, before we get to conduct the out-of-sample analysis, we have to adjust forecasts according to their respective scales as

[6] Parkinson (1980) proposed range with scaling factor $1/\sqrt{4\ln 2}$ as an unbiased estimator for return volatility under the assumption that, during the day, the log-price follows a geometric Brownian motion with zero drift. In other words, return volatility and range relationship is $\sigma = \mathrm{E}(R_t)/\sqrt{4\ln 2}$. However, the relationship is not truly empirical if we consider that the volatilities are serially correlated and thus the independence assumption does not hold. In practice, we replace the constant scaling factor with the coefficient $\hat{\varphi}_r$ from Eq. (25).

follows:

$$\mathrm{MV}_{1+r,k+r} = \varphi_r \cdot \mathrm{FV}_{1+r,k+r}(m) + \nu_{1+r,k+r}\,, \tag{24}$$

$$\mathrm{AFV}_{k+r+h}(m) = \hat{\varphi}_r \cdot \mathrm{FV}_{k+r+h}(m),\ r = 0,1,2,\ldots,s-1\,, \tag{25}$$

where r is the number of adjusting procedures and h is the forecast horizon. The regression is re-estimated at each forecast horizon using a window of k observations indexed $1+r,\ldots,k+r$ (rolling scheme). We proceed in this manner through the end of the out-of-sample period.

4. EMPIRICAL ANALYSIS

This section describes the empirical analysis. We present results of the in-sample analysis in Section 4.1 and those of the out-of-sample analysis in Section 4.2. The robustness checks of those results are provided in Section 4.3. Further analysis is presented in Section 4.4.

4.1 In-Sample Analysis

To support our idea of splitting the low-frequency price range into its continuous and jump components, empirical investigations are conducted on five equity market indices. We collect the daily data of the Australia AORD index (2000/01/04–2020/01/15), the American DJI and S&P 500 indices (2000/01/03–2020/01/15), the Hong Kong HSI index (2000/01/03–2020/01/15), and the Japan NK 225 index (2000/02/02–2020/01/15). Each data set is downloaded from the finance website of "Yahoo.com" for open, high, low and close prices and the publicly available Oxford–Man Institute's Realized Library of Heber et al. (2009) for RV and BPV measures sampled at 5-min intervals. Due to small differences in trading days in different equity markets, the number of observations varies to some degree.

Table 1 summarizes descriptive statistics of three estimators (the high–low range in Panel A, the continuous part in Panel B, and the jump part in Panel C) and the realized volatility used as a benchmark in Panel D. First, range and its components are seriously right-skewed with high kurtosis, indicating a deviation from the normal distribution.[7] Jarque–Bera tests clearly reject the null of a Gaussian distribution in all series. Second, the Ljung–Box Q statistics indicate strong persistence on both the continuous and jump components, especially on the former, which exhibits the best-known volatility clustering effect and is of high predictability, especially for the continuous component. Third, jumps tend to be more volatile than the continuous variation for comparing the standard deviation to the mean, as expected. Accordingly, these preliminary statistical analyses of the data encourage us to use the CARR model of Chou (2005) for range volatility estimation and can be viewed as a primitive indicator of the difference between the dynamic structures of the two components. Fourth, the remaining estimator is considered as a reference. Comparing with the average of the high–low range in the table, the range average is much higher than the realized volatility. This confirms the implementation of the scale factor

[7] The sample kurtosis is above the normal value of 3 for a series, indicating that the distribution of the series is highly leptokurtic (fat tail) due to a few outliers.

TABLE 1
SUMMARY STATISTICS OF DIFFERENT VOLATILITY MEASURES

	AORD	DJI	HSI	NK 225	S&P 500
Panel A: Price range					
Sample size	5,052	5,024	4,901	4,866	5,027
Max.	0.081	0.122	0.176	0.138	0.109
Min.	0.001	0.002	0.003	0.002	0.001
Mean	0.010	0.013	0.014	0.014	0.013
Sd.	0.006	0.010	0.009	0.009	0.010
Skew.	3.014	3.296	3.972	3.579	3.100
Kurt.	20.025	22.472	40.588	28.630	19.836
JB$\times 10^{-3}$	68.661***	88.468***	301.403***	143.575***	67.424***
$Q(12) \times 10^{-2}$	126.452***	201.326***	129.807***	105.967***	212.892***
Panel B: Continuous component					
Max.	0.081	0.108	0.176	0.138	0.109
Min.	0.001	0.002	0.003	0.002	0.001
Mean	0.009	0.011	0.013	0.012	0.012
Sd.	0.006	0.009	0.008	0.009	0.009
Skew.	3.080	3.492	4.222	3.871	3.232
Kurt.	21.024	24.674	47.184	32.867	21.231
JB$\times 10^{-3}$	76.371***	108.551***	413.215***	193.015***	78.369***
$Q(12) \times 10^{-2}$	132.887***	205.143***	126.603***	108.749***	215.726***
Panel C: Jump component					
Max.	0.036	0.088	0.062	0.056	0.070
Min.	0.000	0.000	0.000	0.000	0.000
Mean	0.003	0.005	0.004	0.004	0.005
Sd.	0.003	0.006	0.004	0.004	0.005
Skew.	2.291	3.329	2.856	2.431	3.191
Kurt.	13.368	25.550	21.118	18.604	21.769
JB$\times 10^{-3}$	27.046***	115.727***	73.694***	54.162***	82.316***
$Q(12) \times 10^{-2}$	7.358***	39.003***	22.976***	7.517***	41.438***
Panel D: Realized volatility					
Max.	0.039	0.093	0.066	0.057	0.088
Min.	0.001	0.001	0.002	0.001	0.001
Mean	0.006	0.008	0.009	0.009	0.008
Sd.	0.003	0.006	0.005	0.005	0.006
Skew.	2.889	3.515	3.204	2.758	3.216
Kurt.	17.038	26.851	22.474	17.905	22.174
JB$\times 10^{-3}$	48.509***	129.431***	85.828***	51.217***	85.674***
$Q(12) \times 10^{-2}$	188.187***	260.462***	253.662***	208.475***	287.504***

NOTE: The table reports the summary price range, continuous component, jump component, and realized volatiltiy statistics for the five equity indices listed (Australia AORD, American DJI and S&P 500, Hong Kong HSI, and Japan NK 225). The sample period is from Jan 3, 2000 to Jan 15, 2020. The Jarque–Bera (JB) statistic is used to test the null hypothesis that the series is normally distributed. $Q(k)$ denotes the Ljung–Box Q statistics for k-th order autocorrelation of the series. The numbers of the last two rows of each panel in this table are JB $\times 10^{-3}$ and $Q(k) \times 10^{-2}$. *** denotes significance at the 1% level.

adjustment on range forecasts.[8] As highlighted by Anderson et al. (2000), the realized volatility presents the highest autocorrelation owing to the market microstructure noise.

Figure 1 displays the time series plots of the continuous component in blue and the jumps in red over the sample period. The different dynamics observed in the two parts of the range suggest that there is novel information in this decomposition that might help predict future volatility. To get a better understanding of the contribution of jumps to the price range, following Aït-Sahalia and Jacod (2012), we estimate the relative contribution of the two continuous and jump

[8] Please see footnote 6 above.

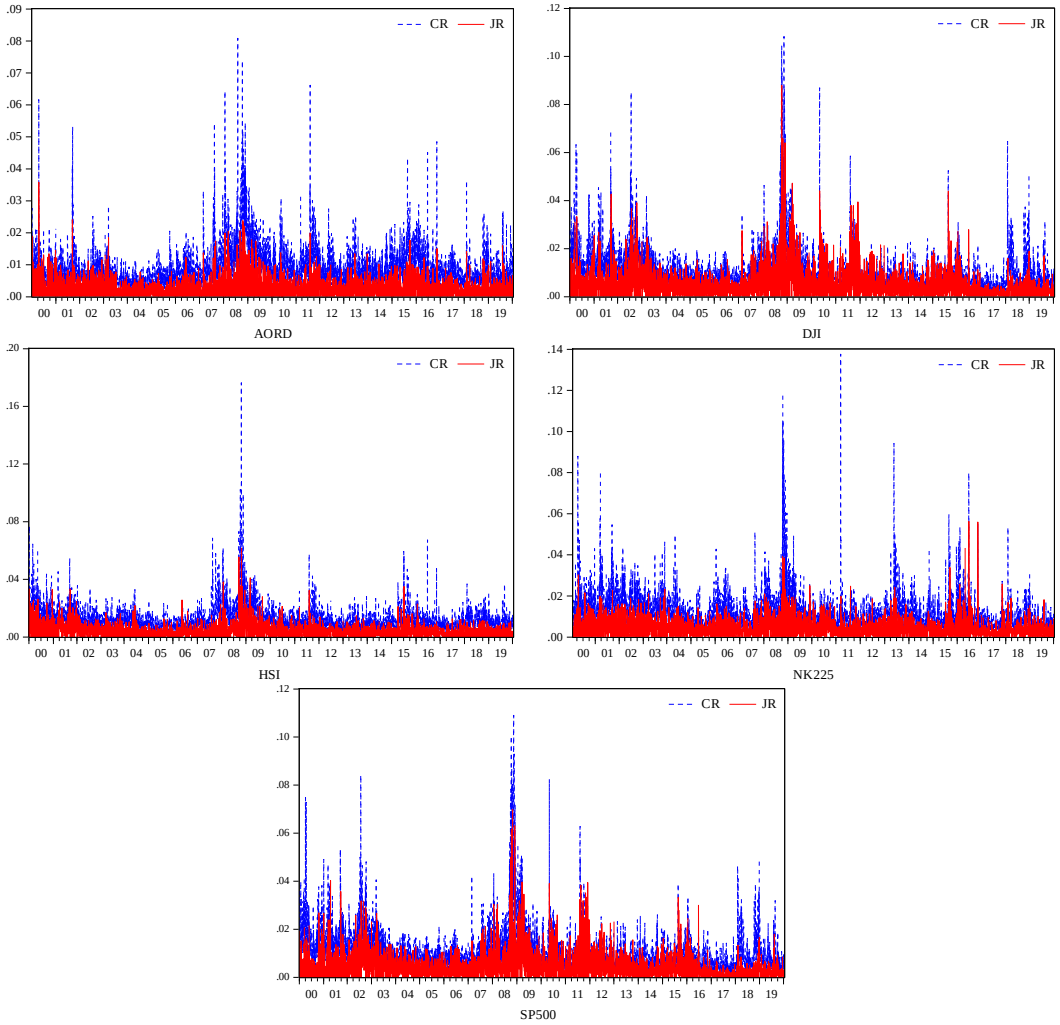

FIG. 1. Time Series of Range − Continuous and Jump Components

NOTE: This figure depicts the continuous and jump elements of the high–low price range for the five equity indices (Australia AORD, American DJI and S&P 500, Hong Kong HSI, and Japan NK 225).

components, respectively, to the squared price range, as defined in Eq. (12):

$$CR(\%) = \frac{CR_t^2}{CR_t^2 + JR_t^2} \times 100, \quad JR(\%) = \frac{JR_t^2}{CR_t^2 + JR_t^2} \times 100. \tag{26}$$

Table 2 reports the percentage contribution of the continuous and jump parts to the squared range for all the equity indices estimated as in Eq. (26). We find that the contribution of the total jumps varies between 11% and 20% and has a mean of about 15.363%, indicating that jumps are an indispensable component of daily equity price movements, in line with the results in Andersen et al. (2007) and Huang and Tauchen (2005).[9] In addition, using the continuous and jump measures, we can also see if the level of the jumps matters in modeling and forecasting volatility on the basis of the range-based model.

Table 3 presents the correlations of the range measures of the five equity markets in the entries below the diagonal of each panel. We find that jumps are relatively highly correlated with both R_t

[9] In Huang and Tauchen (2005) study, the average contribution of total jumps to the total realized variance is about 17.319% for the S&P 500 index futures from April 21, 1982 to April 18, 1997.

TABLE 2

CONTRIBUTION OF THE SQUARED CONTINUOUS AND JUMP COMPONENTS TO THE TOTAL SQUARED PRICE RANGE VARIABILITY

	AORD	DJI	HSI	NK 225	S&P 500	Average
CR(%)	88.958	80.123	86.424	84.873	82.808	84.637
JR(%)	11.042	19.877	13.576	15.127	17.192	15.363

NOTE: This table reports the percent contribution of the daily squared continuous and jump components to the total squared range variability for five equity indices (Australia AORD, American DJI and S&P 500, Hong Kong HSI, and Japan NK 225). The percentages of total price range variation attributable to each component are as follows:

$$CR(\%) = \frac{CR_t^2}{CR_t^2 + JR_t^2} \times 100\,, \quad JR(\%) = \frac{JR_t^2}{CR_t^2 + JR_t^2} \times 100\,.$$

TABLE 3

CORRELATIONS BETWEEN VOLATILITIES OF FIVE EQUITY INDICES

	R_t	CR_t	JR_t
Panel A: AORD			
R_t	1		
CR_t	0.992***	1	
JR_t	0.590***	0.492***	1
Panel B: DJI			
R_t	1		
CR_t	0.968***	1	
JR_t	0.679***	0.489***	1
Panel C: HSI			
R_t	1		
CR_t	0.988***	1	
JR_t	0.597***	0.476***	1
Panel D: NK 225			
R_t	1		
CR_t	0.990***	1	
JR_t	0.549***	0.432***	1
Panel E: S&P 500			
R_t	1		
CR_t	0.977***	1	
JR_t	0.658***	0.499***	1

NOTE: This table reports the correlation between the different range measures for each equity index. *** denotes significance at the 1% level. CR_t and JR_t are the continuous and jump parts of the price range, respectively.

and CR_t at the 1% level of significance. Interestingly, the level of correlation between the total range and the continuous part is somewhat greater than that between the total range and the jump part. The difference levels of correlations observed in price range dissected by the RV and BPV measures suggest that there is novel information in this decomposition that might help predict future volatility.

Results of estimations for the price range and its continuous component (CARR-C) and jump component (CARR-J) together with values of the log-likelihood function (LLF) and the Ljung–Box Q statistics are presented in Table 4. The results show that the asymmetry in the dynamic structures for the continuous and jump parts as values of coefficients α and β in CARR-C and CARR-J models is quite different. On the other hand, the higher values for LLF occur with

TABLE 4
IN-SAMPLE ESTIMATION RESULTS OF CARR MODEL AND CARR-CJ MODEL

	$\omega\times10^4$	α	β	$\alpha+\beta$	Half-life	LLF	Q(12)
Panel A: AORD							
CARR	1.877(0.000)	0.153(0.000)	0.828(0.000)	0.980	35.779	187.107	15.249(0.228)
CARR-C	1.799(0.000)	0.159(0.000)	0.821(0.000)	0.980	35.108	187.116	15.682(0.206)
CARR-J	0.260(0.001)	0.035(0.000)	0.955(0.000)	0.990	67.328		
Panel B: DJI							
CARR	2.321(0.000)	0.209(0.000)	0.773(0.000)	0.981	38.044	174.489	19.815(0.071)
CARR-C	2.537(0.000)	0.231(0.000)	0.746(0.000)	0.977	30.368	174.526	19.112(0.086)
CARR-J	0.314(0.002)	0.068(0.000)	0.926(0.000)	0.994	111.609		
Panel C: HIS							
CARR	1.718(0.000)	0.113(0.000)	0.874(0.000)	0.987	53.294	164.522	16.963(0.151)
CARR-C	1.768(0.000)	0.119(0.000)	0.866(0.000)	0.985	48.166	164.522	15.133(0.236)
CARR-J	0.291(0.001)	0.039(0.000)	0.954(0.000)	0.992	92.358		
Panel D: NK 225							
CARR	3.644(0.000)	0.197(0.000)	0.776(0.000)	0.973	26.592	164.089	45.569(0.000)
CARR-C	3.365(0.000)	0.202(0.000)	0.771(0.000)	0.973	26.518	164.097	46.686(0.000)
CARR-J	0.360(0.004)	0.045(0.000)	0.947(0.000)	0.992	85.607		
Panel E: S&P 500							
CARR	2.544(0.000)	0.216(0.000)	0.763(0.000)	0.980	34.892	174.080	27.061(0.008)
CARR-C	2.850(0.000)	0.235(0.000)	0.739(0.000)	0.974	27.783	174.110	23.367(0.025)
CARR-J	0.250(0.001)	0.068(0.000)	0.926(0.000)	0.995	131.808		

NOTE: The CARR model $\lambda_t=\omega+\alpha R_{t-1}+\beta\lambda_{t-1}$, where R_t is the price range. The CARR-CJ model $\lambda_t^C=\omega^C+\alpha^C CR_{t-1}+\beta^C\lambda_{t-1}^C$ and $\lambda_t^J=\omega^J+\alpha^J JR_{t-1}+\beta^J\lambda_{t-1}^J$, where CR_t and JR_t are the continuous and jump parts of the price range, respectively. Both CARR and CARR-CJ models are estimated using the QMLE method. LLF is the log likelihood function and is multiplied by 10^{-2}. $Q(k)$ is the Ljung-Box Q statistic for the autocorrelation test with k lags. Numbers in parentheses are p-values for model coefficients and Q(k) statistic.

the newly proposed CARR-CJ model, indicating that the CARR-CJ model fit improves compared with the CARR model. The Ljung–Box Q test statistics with 12 lags ($Q(12)$) reveal a serial correlation in residuals at the 5% level of significance, except for AORD, DJI, and HSI in both models, indicating that there is information left in the residuals that should be used for computing forecasts. A possible consideration for inclusion is the leverage effect of Black (1976) and Nelson (1991). As is well known, the lagged asset return contributes to forecasting of financial volatility. If the dynamics of both range and its components depend on the lagged asset return, the leverage effect can capture the serial correlation in residuals and reduce the value of $Q(12)$ statistic. We subsequently test this hypothesis by taking into consideration the leverage effect (see Section 4.3).

It is more interesting to compare the results of the CARR-C model with those of the CARR-J model. First, the persistence parameter, measured by $\alpha+\beta$, is higher for the jump component than for the continuous component by about 0.7%–2.2%. We take a look at the volatility half-life of Engle and Patton (2001) and find that the jumps take the longest days to revert back to half of their mean, indicating that the price jump has a significant impact on the long-run forecast of the volatility.[10] Taking the S&P 500 equity index as an example, the half-life of the price range, continuous part, and jump part is 35, 28, and 132 days, respectively. This means that a shock in jump will take 132 days for the jump volatility to return half way back to its mean value. Second, the shock effect in the short-run, measured by the coefficient α, is much lower for the jump

[10] Engle and Patton (2001) defined half-life as the time required for the volatility to move half way back toward its unconditional mean.

TABLE 5
MAE, RMSE, AND QLIKE STATISTICS OF IN-SAMPLE FORECASTS BY CARR AND CARR-CJ

	MAE	RMSE	QLIKE
Panel A: AORD			
CARR	0.405	0.473	15.954
CARR-CJ	0.386	0.452	15.104
Ratio	**0.954**	**0.957**	**0.947**
Panel B: DJI			
CARR	0.473	0.600	12.688
CARR-CJ	0.435	0.551	11.675
Ratio	**0.921**	**0.919**	**0.920**
Panel C: HSI			
CARR	0.521	0.607	12.418
CARR-CJ	0.491	0.573	11.599
Ratio	**0.943**	**0.945**	**0.934**
Panel D: NK 225			
CARR	0.506	0.603	12.103
CARR-CJ	0.480	0.573	11.442
Ratio	**0.948**	**0.950**	**0.945**
Panel E: S&P 500			
CARR	0.492	0.619	13.361
CARR-CJ	0.458	0.573	12.436
Ratio	**0.931**	**0.927**	**0.931**

NOTE: This table computes the MAE, RMSE, and QLIKE using the following equations:

$$\mathrm{MAE}(m)=T^{-1}\sum_{t=1}^{T}\left|\mathrm{MV}_t-\mathrm{FV}_t(m)\right|,\quad \mathrm{RMSE}(m)=\left[T^{-1}\sum_{t=1}^{T}\left(\mathrm{MV}_t-\mathrm{FV}_t(m)\right)\right]^{0.5},\quad \mathrm{QLIKE}(m)=T^{-1}\sum_{t=1}^{T}\left(\frac{\mathrm{MV}_t}{\mathrm{FV}_t(m)}-\ln\left(\frac{\mathrm{MV}_t}{\mathrm{FV}_t(m)}\right)-1\right),$$

where MV_t and $\mathrm{FV}_t(m)$ are, respectively, the measure of volatility and the predictions reported by model m. Entries in bold indicate that the CARR-CJ model outperforms the CARR model. The MAE, RMSE, and QLIKE reported in this table have been multiplied by 100.

component than for the continuous component, by about 67.2%–78.0%. Taking the Australia AORD equity index as an example, the shock effect in the CARR-C model declines 78%, from 0.159 to 0.035, in the CARR-J model. These results suggest that the jump component has a longer half-life and smaller short-run impact on future volatility compared to the continuous component. Third, the coefficients α for the CARR-C model are somewhat higher than their corresponding elements in the standard CARR model. This seems to indicate that the continuous component is a less noisy volatility proxy than the price range as we have removed noise (jumps) from the continuous component in the volatility proxy, which is consistent with the finding in Corsi et al. (2010).

To the best of our knowledge, the abovementioned findings are new in the literature on range-based models as no existing studies distinguish the shock asymmetry in this fashion. Moreover, the message from this section is clear: the dynamic evolutions of the continuous and jump components are relatively different. They are different in their dynamics of the volatility shocks, i.e., the short-run impact and volatility persistence. Note that the Ljung–Box Q statistics show that neither CARR nor CARR-CJ model for NK 225 and S&P 500 is sufficient; thus, exogenous variables might be necessary to assure a model passes misspecification tests.

Although the above empirical results suggest explicit differences between models for the continuous and jump components, we further examine if the separation of the price range into its two parts is useful to predict financial volatility. In view of the return-based analysis, Corsi et al.

TABLE 6
IN-SAMPLE COMPARISON FOR CARR-CJ VERSUS CARR ON REALIZED VOLATILITY

	Explanatory variables			
Measured volatility	**Constant** $\times 10^4$	**FV(CARR)**	**FV(CARR-CJ)**	**Adj.** R^2 **(%)**
Panel A: AORD				
σ_{RV}	−1.086(0.502)	0.615(0.000)		53.888
σ_{RV}	−1.477(0.370)		0.633(0.000)	54.263
σ_{RV}	−1.637(0.333)	−0.784(0.001)	1.436(0.000)	54.426
Panel B: DJI				
σ_{RV}	−1.571(0.417)	0.673(0.000)		66.748
σ_{RV}	−4.050(0.048)		0.717(0.000)	67.546
σ_{RV}	−4.797(0.046)	−0.300(0.134)	1.033(0.000)	67.623
Panel C: HSI				
σ_{RV}	−1.612(0.566)	0.647(0.000)		64.031
σ_{RV}	−2.803(0.317)		0.671(0.000)	64.263
σ_{RV}	−3.614(0.202)	−0.541(0.107)	1.232(0.000)	64.316
Panel D: NK 225				
σ_{RV}	2.318(0.147)	0.633(0.000)		60.784
σ_{RV}	1.218(0.476)		0.656(0.000)	60.811
σ_{RV}	1.624(0.347)	0.274(0.198)	0.372(0.092)	60.841
Panel E: S&P 500				
σ_{RV}	−1.728(0.351)	0.658(0.000)		70.108
σ_{RV}	−3.680(0.051)		0.694(0.000)	70.806
σ_{RV}	−4.420(0.033)	−0.369(0.041)	1.080(0.000)	70.903

NOTE: In-sample volatility forecasts comparison using realized volatility (σ_{RV}) as a measured volatility. Numbers in parentheses are heteroskedasticity and autocorrelation consistent (HAC) p-values. For the forecast regression analysis,

$$MV_t = a + bFV_t(m) + u_t,$$

where MV_t and FV_t (m) are the measure of volatility and the predictions reported by model m, respectively. For the forecast encompassing regression analysis,

$$MV_t = a + bFV_t(\text{CARR}) + cFV_t(\text{CARR - CJ}) + u_t.$$

(2010) showed that jumps had a positive and mostly significant impact on future volatility, and that the performance of the volatility model that explicitly incorporated the jumps was significantly improved. Similar results were also obtained by Andersen et al. (2007). Accordingly, in this section, we further compare the forecasting power of the standard CARR model with that of the CARR-CJ model, which considers the jumps. Given our new findings of the different dynamics of the two components, we would expect the CARR-CJ model to perform better than the standard CARR model in terms of both in-sample fit and out-of-sample forecasting ability.

As for in-sample performance, we use the entire sample to produce forecasts with the competing models. Table 5 reports the in-sample MAE, RMSE, and QLIKE. Panels A to E report the MAE, RMSE, and QLIKE separately for both the CARR and CARR-CJ models across the five equity indices we have considered. For the CARR-CJ model, the range forecasts are obtained by adding the squared continuous forecasts to the squared jump forecasts first and then taking the square root, as shown in Eq. (12). We also calculate the ratio of MAE (RMSE, QLIKE) reported by the CARR- CJ model to the MAE (RMSE, QLIKE) reported by the CARR model. The ratio provides the relative performance of the CARR-CJ model to the CARR model. If the ratio is smaller than one, then the CARR-CJ model outperforms the CARR model in the in-sample fit of

the data. Consistently, the in-sample forecasting results show that the CARR-CJ is the best performing model in all five equity indices; the three criteria and the ratio statistics show that the CARR-CJ model makes smaller errors than the CARR model in forecasting the 5-min realized volatility (σ_{RV}), as defined in Eq. (20). Hence, by exploiting the differences in the dynamic structures of these two movements to generate volatility forecasts, the CARR-CJ model delivers the best forecasts.

To get further insights into the difference between the CARR-CJ and CARR models, we use regression-based tests to assess the ability of these two competing models to predict realized volatility. In addition to examination for coefficients, we also examine the regression R^2's. Table 6 presents the regression results on realized volatility. The results clearly show the uniform superiority of the CARR-CJ model as follows: (1) the encompassing regression results show the dominance of the CARR-CJ model over the CARR model. Once the forecasts reported by the CARR-CJ model are included, the forecasts reported by the CARR model provide insignificant explanatory power or have a negative coefficient; (2) forecasts given by the CARR-CJ model are more informative than those by the CARR model as the adjusted R^2 statistics of the CARR-CJ model are higher than those of the CARR model in all cases.

4.2 Out-of-Sample Analysis

Out-of-sample forecasting performance is crucial to the market participants. Following Chou (2005), we perform out-of-sample forecasting using the rolling window approach. For each equity index, we split the whole data set into an in-sample set (60%) and an out-of-sample set (40%). We employ one-step- and multi-step-ahead forecasts because it is useful to compare the selected models at longer horizons. The forecast horizons (h) range from 1 to 66 days (one quarter). The first end date is December 1, 2011 (AORD), January 11, 2012 (DJI), January12, 2012 (HSI), January 26, 2012 (NK 225), and January 12, 2012 (S&P 500), whereas the last end date is October 10, 2019 (AORD), Octocber10, 2019 (DJI), October 10, 2018 (HSI), October 3, 2019 (NK 225), and October 8, 2019 (S&P 500). Following Patton (2011), we focus on the RMSE and QLIKE criteria, as both criteria are more robust to noisy proxy of the latent volatility than others.[11] Table 7 presents the RMSE, QLIKE, and DM statistics for the CARR and CARR-CJ models with respect to realized volatility. We report five forecast horizons with daily (1 day ahead), weekly (5 days ahead), monthly (22 days ahead), bi-monthly (44 day ahead), and quarterly (66 days ahead) only, in order to save space.[12] The results for the five equity indices are reported separately across the five horizons we consider. The bottom rows report the list of the models and the fraction of times a given model is best across the five equity indices for a given horizon. From Table 7, we note that across horizons and equity indices, the CARR-CJ model is the best performing model in 100% of the cases using the RMSE and QLIKE criteria. Besides, 24 out of 25 or 96% of the cases show that the CARR-CJ model's RMSE is statistically lower than that of the CARR model at the

[11] A robust criterion yields rankings of competing volatility forecasts to be robust to the noise in the volatility proxy (see Patton, 2011).

[12] Results for remaining forecast horizons are available upon request.

TABLE 7

RMSE AND QLIKE STATISTICS OF THE OUT-OF-SAMPLE FORECASTS ON REALIZED VOLATILITY BY CARR AND CARR-CJ: ROLLING WINDOW APPROACH

	RMSE					QLIKE				
	Horizon (days)					Horizon (days)				
	1	**5**	**22**	**44**	**66**	**1**	**5**	**22**	**44**	**66**
Panel A: AORD										
CARR	0.201	0.222	0.242	0.247	0.255	4.837	5.902	7.313	7.762	8.327
CARR-CJ	0.200	0.220	0.240	0.245	0.252	4.815	5.872	7.216	7.613	8.137
Ratio	**0.996**	**0.994**	**0.992**	**0.990**	**0.988**	**0.995**	**0.995**	**0.987**	**0.981**	**0.977**
DM stat.	−1.991**	−2.362**	−3.868***	−4.903***	−6.194***	−1.069	−0.779	−2.937***	−4.699***	−5.995***
Panel B: DJI										
CARR	0.293	0.350	0.397	0.416	0.432	6.113	9.112	13.225	15.074	16.545
CARR-CJ	0.290	0.345	0.386	0.402	0.413	5.960	8.965	12.688	14.240	15.398
Ratio	**0.991**	**0.986**	**0.972**	**0.965**	**0.957**	**0.975**	**0.984**	**0.959**	**0.945**	**0.931**
DM stat.	−1.138	−2.211**	−4.847***	−6.070***	−8.782***	−2.181**	−1.275	−5.573***	−6.420***	−8.261***
Panel C: HSI										
CARR	0.223	0.249	0.274	0.277	0.294	3.642	4.434	5.552	5.974	6.824
CARR-CJ	0.220	0.246	0.269	0.272	0.288	3.529	4.324	5.400	5.738	6.536
Ratio	**0.985**	**0.986**	**0.984**	**0.979**	**0.977**	**0.969**	**0.975**	**0.973**	**0.960**	**0.958**
DM stat.	−5.080***	−3.662***	−4.378***	−7.225***	−8.608***	−6.943***	−4.233***	−4.465***	−7.958***	−9.049***
Panel D: NK 225										
CARR	0.317	0.369	0.422	0.436	0.447	5.208	7.620	11.062	12.185	13.007
CARR-CJ	0.315	0.364	0.416	0.429	0.439	5.133	7.470	10.725	11.721	12.487
Ratio	**0.993**	**0.988**	**0.986**	**0.983**	**0.981**	**0.986**	**0.980**	**0.970**	**0.962**	**0.960**
DM stat.	−2.019**	−2.833***	−5.372***	−6.574***	−7.939***	−2.701***	−2.915***	−4.984***	−6.750***	−7.944***
Panel E: S&P 500										
CARR	0.265	0.328	0.378	0.400	0.419	6.163	9.498	13.752	15.870	17.519
CARR-CJ	0.261	0.322	0.367	0.386	0.400	5.991	9.305	13.210	15.025	16.346
Ratio	**0.985**	**0.982**	**0.971**	**0.964**	**0.955**	**0.972**	**0.980**	**0.961**	**0.947**	**0.933**
DM stat.	−2.557**	−3.252***	−4.982***	−6.626***	−9.986***	−3.373***	−2.342**	−6.054***	−7.158***	−9.431***
Model	*Fraction of times a model is the best*									
CARR	0%	0%	0%	0%	0%	0%	0%	0%	0%	0%
CARR-CJ	100%	100%	100%	100%	100%	100%	100%	100%	100%	100%

NOTE: This table computes the RMSE and QLIKE using the following equations:

$$\text{RMSE}(m,h)=\left[T^{-1}\sum_{t=1}^{T}\left(\text{MV}_{t+h}-\text{FV}_{t+h}(m)\right)\right]^{0.5},\quad \text{QLIKE}(m,h)=T^{-1}\sum_{t=1}^{T}\left(\frac{\text{MV}_{t+h}}{\text{FV}_{t+h}(m)}-\ln\left(\frac{\text{MV}_{t+h}}{\text{FV}_{t+h}(m)}\right)-1\right),$$

where MV_t and $\text{FV}_t(m)$ are the measure of volatility and the predictions reported by model m, respectively. All tests are out-of-sample and carried out using the rolling window approach. We only report cases with h =1, 5, 22, 44, and 66 days. Smaller RMSE (QLIKE) means lower forecasting error. Bold entries and negative values of the DM test indicate that the CARR-CJ model beats the CARR model. The RMSE and QLIKE reported in this table have been multiplied by 100. The bottom rows report the list of models and the fraction of times a given model is best across the five equity indices for a given horizon. ***, **, and * represent 1%, 5%, and 10% levels of significance, respectively.

10% level; whereas 22 out of 25 or 88% of the cases show the CARR-CJ model's QLIKE is statistically lower than that of the CARR model at the 10% level.[13] An interesting finding is that the CARR-CJ model delivers rather superior performances at longer horizons since the ratio statistics decrease with the forecast horizons. Taking the S&P 500 equity index as an example, the ratio statistic is 0.985 (0.972) at the 1-day horizon and 0.955 (0.933) at the 66-day horizon using the RMSE (QLIKE) criterion. Consistent with the ratio statistics, the DM statistics are much larger and more significant at longer horizons than those at shorter horizons in all cases. The reason for

[13] Ahoniemi and Lanne (2013) ran the Diebold–Mariano test to examine if a realized volatility estimator incorporating overnight information is more accurate for thirty equities in the US stock market with a 10% confidence level.

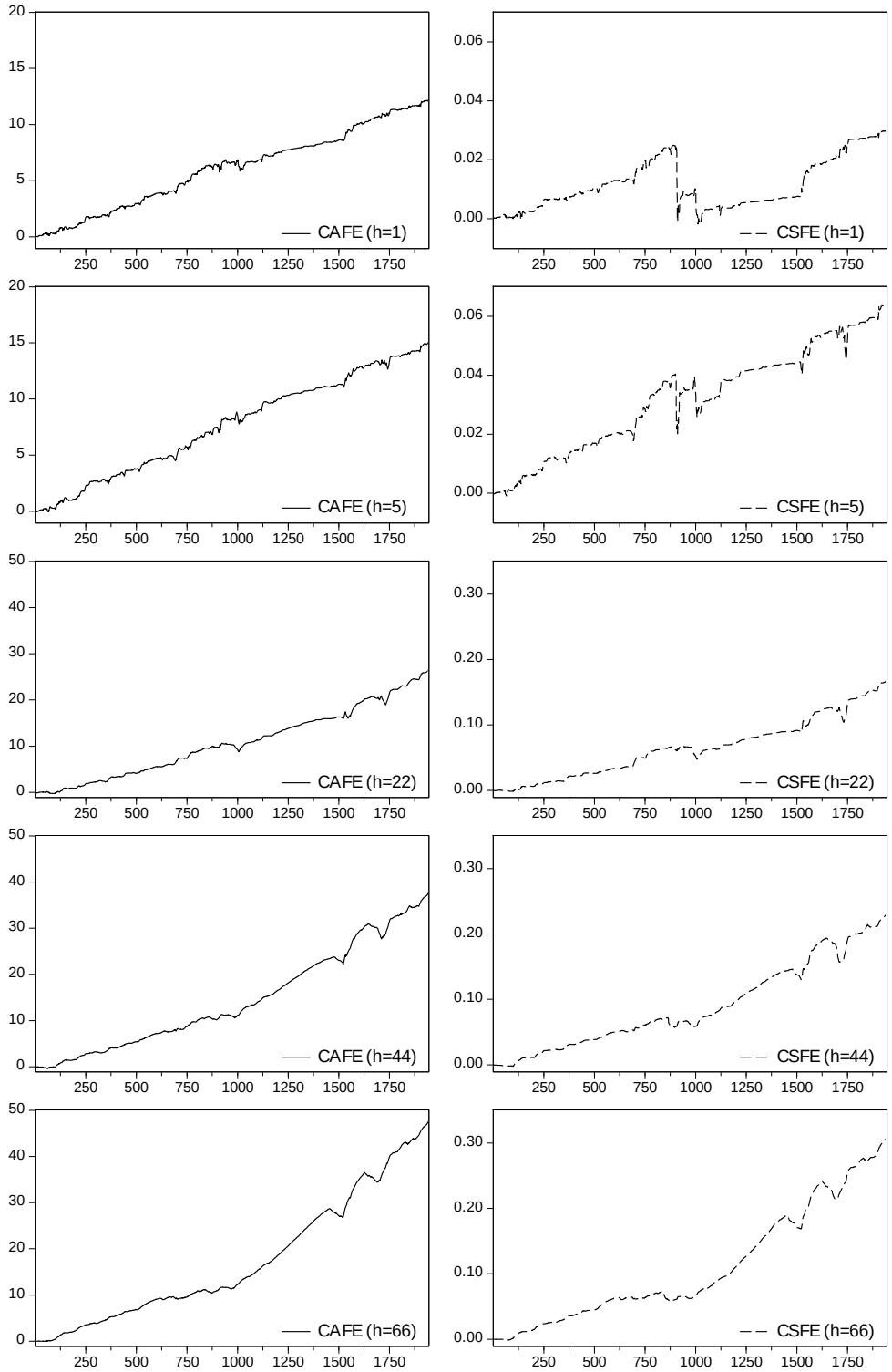

FIG. 2. Cumulative Absolute and Squared Forecast Error Differences (American DJI Index)

NOTE: This figure depicts the cumulative absolute forecast error (CAFE) difference and cumulative squared forecast error (CSFE) difference for the range forecasts using the CARR and CARR-CJ models. CAFE difference and CSFE difference are defined, respectively, as follows:

$$\text{CAFE}_t = \sum_{k=1}^{t} \left(\left| \text{MV}_k - \text{FV}_k(\text{CARR}) \right| - \left| \text{MV}_k - \text{FV}_k(\text{CARR - CJ}) \right| \right),$$

$$\text{CSFE}_t = \sum_{k=1}^{t} \left[(\text{MV}_k - \text{FV}_k(\text{CARR}))^2 - (\text{MV}_k - \text{FV}_k(\text{CARR - CJ}))^2 \right],$$

where MV_k is the measure of volatility and FV_k is the prediction reported by the CARR and CARR-CJ models. If the curve increases, the CARR-CJ model outperforms the CARR model, whereas the opposite holds if the curve decreases.

this result is that since the possibility of occurrence of jumps at longer horizons is higher than at shorter horizons, the CARR-CJ model could largely improve the forecasting power on realized volatility in the days following a jump; thus, the fact that the CARR-CJ model slightly outperforms the CARR model at shorter horizons is not surprising as the difference between the two forecasts is primarily during the days following a jump, which may be few at shorter horizons.

To comprehensively examine the relative contribution afforded by the CARR-CJ model, following Welch and Goyal (2008), we use the out-of-sample forecast errors to compute the cumulative absolute forecast errors (CAFE) difference and the cumulative squared forecast errors (CSFE) difference for the CARR and CARR-CJ models. The CAFE and CSFE differences are defined, respectively, as follows:

$$\text{CAFE}_t = \sum_{k=1}^{t} \left(\left| \text{MV}_k - \text{FV}_k(\text{CARR}) \right| - \left| \text{MV}_k - \text{FV}_k(\text{CARR - CJ}) \right| \right), \tag{27}$$

$$\text{CSFE}_t = \sum_{k=1}^{t} \left[(\text{MV}_k - \text{FV}_k(\text{CARR}))^2 - (\text{MV}_k - \text{FV}_k(\text{CARR - CJ}))^2 \right]. \tag{28}$$

Positive and increasing values of CAFE_t or CSFE_t suggest that the CARR-CJ model's predictability generates more accurate forecasts than the CARR benchmark with the time varying. Figure 2 plots CAFE_t, shown in solid line, and CSFE_t, shown in dashed line, on different forecast horizons using realized volatility as a reference. Because of space constraints, we only present the cases on the American DJI index for five forecast horizons, i.e., h = 1, 5, 22, 44, and 66 days.[14] With such graphical analysis, we can visually inspect the predictive performance of each model on different forecast horizons. These plots show that the CARR- CJ model beats the CARR model in forecasting the realized volatility across horizons. However, a closer look at the plots reveals something interesting. For the longer horizons, the curve has a plot that is always increasing and well-above zero, which means the CARR-CJ model consistently outperforms the CARR benchmark over the whole out-of-sample periods. In contrast to the shorter horizons, the curve decreases even below zero for some periods, which means the CARR-CJ model underperforms compared with the CARR model for some time. Figure 2 visually provides a very important message: a range model with separation of the continuous and jump components largely improves the forecasting power at longer horizons because of the frequent occurrence of jumps, which further confirms the forecast comparison results in Table 7. Similar performances are also seen for other equity indices; however, we do not present these graphs here.

Overall, in-sample and out-of-sample evidence show that the CARR-CJ model outperforms the CARR model. The conclusion of this section is clear: separating dynamic structures for continuous and jump components of the price range yields a substantial improvement in volatility forecasting, especially at longer horizons, as we allow separate dynamic structures for the two components of asset prices to account for asymmetric behaviors in the financial market. To the best of our knowledge, this is a novel empirical finding that further confirms the importance of jumps in financial econometrics.

[14] The CAFE and CSFE plots for other equity indices are available upon request.

4.3 Robustness Check

This paper chooses the realized volatility as a measure of volatility; however, it is sometimes unavailable and is contaminated by market microstructure noise (Anderson et al., 2000). For robustness, we also compare CARR with CARR-CJ using the GK volatility estimator of Garman and Klass (1980) due to the data availability. Formally, the GK estimator is defined as follows:

$$\sigma_{GK} = \sqrt{0.5[p_t^H - p_t^L]^2 - (2\ln 2 - 1)[p_t^C - p_t^O]^2}\,, \tag{29}$$

where p_t^C and p_t^O stand for the close and open prices at time t, respectively. Garman and Klass (1980) reported that their estimator is 7.4 times more efficient than a simple close-to-close variance estimator. The efficiency gain can be intuitively attributed to the fact that an estimate also incorporates open and close data besides high and low prices. Hansen and Lunde (2006) suggested range-based estimators might be possible alternative proxies for true volatility, e.g., see Molnár (2016).

Table 8 reports the RMSE, QLIKE, and DM statistics with respect to the GK estimator. The evidence is completely consistent with the results of Table 7. The RMSE and QLIKE statistics show the dominance of the CARR-CJ model over the CARR model. It is clear from the ratio statistics that the CARR-CJ model performs better at longer horizons. Consistent with the ratio statistics, the DM statistics are uniformly reported to be larger and more significant at longer horizons than that at shorter horizons.

It is important to use different forecast schemes to examine robustness of forecasting ability and assess the model performance. Therefore, the recursive (expanding) window estimation method is used.[15] Out-of-sample forecasting is also performed on the equity indices over different time horizons, and the results are reported in Table 9 for realized volatility forecasts. The format is the same as that of Table 8, including the rows that report the fraction of equity indices for which a given model is the best. From Table 9, it can be seen that the CARR-CJ model performs better than the CARR model and over longer horizons.

In empirical studies, equity and stock-index volatilities display a significant asymmetric response to past returns; this so-called "leverage effect" was first noted by Black (1976). To avoid omitted variable bias and investigate the robustness of the forecasting performance, following Chen et al. (2013), we take into account leverage effects on the conditional range by performing the following models:

$$\lambda_t = \omega + \alpha R_{t-1} + \beta\lambda_{t-1} + \gamma I(r_{t-1} < 0) R_{t-1}, \tag{30}$$

[15] To be specific, the whole T data observations are divided into an in-sample portion composed of the first k observations and an out-of-sample portion composed of the last s observations. The initial h-step ahead out-of-sample forecasts FV_{k+h} is based on the first k observations. The sample is increased by one, the models are re-estimated, and the next h-step ahead out-of-sample forecasts produced are based on the first $k + 1$ observations. This process continues until the out-of-sample covers all available data. The recursive predicting procedure simulates the situation of a forecaster in real time (Xie, 2019).

TABLE 8

RMSE AND QLIKE STATISTICS OF THE OUT-OF-SAMPLE FORECASTS ON THE GK ESTIMATOR BY CARR AND CARR-CJ: ROLLING WINDOW APPROACH (ROBUSTNESS CHECK)

	RMSE					QLIKE				
	Horizon (days)					Horizon (days)				
	1	**5**	**22**	**44**	**66**	**1**	**5**	**22**	**44**	**66**
Panel A: AORD										
CARR	0.214	0.227	0.242	0.246	0.253	7.340	8.163	9.457	9.923	10.598
CARR-CJ	0.213	0.226	0.240	0.244	0.251	7.287	8.112	9.345	9.755	10.391
Ratio	**0.995**	**0.993**	**0.993**	**0.991**	**0.990**	**0.993**	**0.994**	**0.988**	**0.983**	**0.980**
DM stat.	−3.129***	−3.059***	−4.405***	−5.573***	−6.702***	−2.367**	−1.373	−3.373***	−5.356***	−6.475***
Panel B: DJI										
CARR	0.273	0.315	0.348	0.364	0.376	8.775	11.524	14.982	16.612	18.028
CARR-CJ	0.270	0.313	0.342	0.355	0.364	8.637	11.454	14.624	16.019	17.163
Ratio	**0.989**	**0.992**	**0.982**	**0.976**	**0.968**	**0.984**	**0.994**	**0.976**	**0.964**	**0.952**
DM stat.	−2.168**	−1.514	−3.161***	−4.360***	−6.699***	−2.360**	−0.705	−3.285***	−4.094***	−5.654***
Panel C: HSI										
CARR	0.298	0.314	0.329	0.330	0.342	6.963	7.618	8.543	8.786	9.521
CARR-CJ	0.298	0.314	0.328	0.328	0.338	6.945	7.606	8.498	8.652	9.335
Ratio	**0.998**	**0.998**	**0.995**	**0.992**	**0.989**	**0.997**	**0.998**	**0.995**	**0.985**	**0.981**
DM stat.	−1.159	−1.065	−1.851*	−3.839***	−5.523***	−0.871	−0.369	−1.109	−3.899***	−5.140***
Panel D: NK 225										
CARR	0.360	0.393	0.426	0.435	0.442	9.036	11.054	13.803	14.686	15.373
CARR-CJ	0.359	0.390	0.423	0.431	0.437	9.008	10.984	13.586	14.351	14.976
Ratio	**0.997**	**0.994**	**0.993**	**0.991**	**0.989**	**0.997**	**0.994**	**0.984**	**0.977**	**0.974**
DM stat.	−1.144	−1.937*	−3.505***	−4.677***	−5.830***	−0.814	−1.245	−3.026***	−4.645***	−5.821***
Panel E: S&P 500										
CARR	0.261	0.306	0.341	0.357	0.371	9.107	11.945	15.389	17.114	18.592
CARR-CJ	0.258	0.303	0.335	0.348	0.358	8.989	11.829	15.004	16.487	17.681
Ratio	**0.989**	**0.989**	**0.981**	**0.975**	**0.967**	**0.987**	**0.990**	**0.975**	**0.963**	**0.951**
DM stat.	−2.488**	−2.216**	−3.425***	−4.911***	−7.798***	−2.436**	−1.447	−3.780***	−4.810***	−6.841***
Model	*Fraction of times a model is the best*									
CARR	0%	0%	0%	0%	0%	0%	0%	0%	0%	0%
CARR-CJ	100%	100%	100%	100%	100%	100%	100%	100%	100%	100%

NOTE: This table computes the RMSE and QLIKE using the following equations:

$$\text{RMSE}(m,h)=\left[T^{-1}\sum_{t=1}^{T}\left(\text{MV}_{t+h}-\text{FV}_{t+h}(m)\right)\right]^{0.5},\quad \text{QLIKE}(m,h)=T^{-1}\sum_{t=1}^{T}\left(\frac{\text{MV}_{t+h}}{\text{FV}_{t+h}(m)}-\ln\left(\frac{\text{MV}_{t+h}}{\text{FV}_{t+h}(m)}\right)-1\right),$$

where MV_t and $\text{FV}_t(m)$ are the measure of volatility and the predictions reported by model m, respectively. All tests are out-of-sample and carried out using the rolling window approach. We only report cases with h =1, 5, 22, 44, and 66 days. Smaller RMSE (QLIKE) means lower forecasting error. Bold entries and negative values of the DM test indicate that the CARR-CJ model beats the CARR model. The RMSE and QLIKE reported in this table have been multiplied by 100. The bottom rows report the list of models and the fraction of times a given model is best across the five equity indices for a given horizon. ***, **, and * represent 1%, 5%, and 10% levels of significance, respectively.

$$\lambda_t^C=\omega^C+\alpha^C CR_{t-1}+\beta^C\lambda_{t-1}^C+\gamma^C I(r_{t-1}<0)CR_{t-1}, \tag{31}$$

$$\lambda_t^J=\omega^J+\alpha^J JR_{t-1}+\beta^J\lambda_{t-1}^J+\gamma^J I(r_{t-1}<0)JR_{t-1}, \tag{32}$$

where r_t is a daily log return in day t and the index function $I(.)$ = 1 when the return r_t is negative; otherwise, $I(.)$ = 0. We denote Eq. (30) as the CARRX model and Eqs. (31) and (32) as the CARRX-CJ model. In the CARRX and CARRX-CJ models, good news is given by $r_t > 0$, and bad news is given by $r_t < 0$. Good news has an impact of γ, γ^C, and γ^J, while bad news has an impact of $\alpha+\gamma$, $\alpha^C+\gamma^C$, and $\alpha^J+\gamma^J$. If γ, γ^C, and γ^J are positive, bad news produces more volatility, an indication of leverage effect.

TABLE 9

RMSE AND QLIKE STATISTICS OF THE OUT-OF-SAMPLE FORECASTS ON REALIZED VOLATILITY BY CARR AND CARR-CJ: EXPANDING WINDOW APPROACH (ROBUSTNESS CHECK)

	RMSE					QLIKE				
	Horizon (days)					Horizon (days)				
	1	**5**	**22**	**44**	**66**	**1**	**5**	**22**	**44**	**66**
Panel A: AORD										
CARR	0.201	0.221	0.238	0.239	0.244	4.845	5.887	7.015	7.183	7.568
CARR-CJ	0.200	0.220	0.237	0.238	0.243	4.848	5.899	6.991	7.121	7.471
Ratio	**0.998**	**0.996**	**0.996**	**0.996**	**0.995**	1.001	1.002	**0.997**	**0.991**	**0.987**
DM stat.	−1.062	−1.407	−1.673*	−1.633	−2.348**	0.124	0.281	−0.636	−1.630	−2.473**
Panel B: DJI										
CARR	0.293	0.347	0.398	0.420	0.438	6.086	9.017	13.105	15.076	16.803
CARR-CJ	0.292	0.344	0.388	0.407	0.422	5.990	8.916	12.666	14.395	15.899
Ratio	**0.996**	**0.990**	**0.977**	**0.969**	**0.964**	**0.984**	**0.989**	**0.966**	**0.955**	**0.946**
DM stat.	−0.530	−1.718*	−5.246***	−6.842***	−9.323***	−1.320	−0.864	−5.307***	−6.992***	−9.255***
Panel C: HSI										
CARR	0.225	0.251	0.276	0.281	0.299	3.714	4.497	5.615	6.068	6.959
CARR-CJ	0.222	0.247	0.271	0.274	0.291	3.588	4.371	5.449	5.813	6.646
Ratio	**0.984**	**0.984**	**0.982**	**0.977**	**0.974**	**0.966**	**0.972**	**0.970**	**0.958**	**0.955**
DM stat.	−5.090***	−3.950***	−4.781***	−7.578***	−9.056***	−7.368***	−4.709***	−4.824***	−8.458***	−9.563***
Panel D: NK 225										
CARR	0.318	0.369	0.426	0.443	0.458	5.222	7.536	11.062	12.504	13.629
CARR-CJ	0.316	0.364	0.419	0.434	0.447	5.159	7.388	10.696	11.956	12.992
Ratio	**0.993**	**0.987**	**0.984**	**0.980**	**0.977**	**0.988**	**0.980**	**0.967**	**0.956**	**0.953**
DM stat.	−1.791*	−2.955***	−5.721***	−7.750***	−9.464***	−2.063**	−2.785***	−5.229***	−7.932***	−9.482***
Panel E: S&P 500										
CARR	0.265	0.325	0.377	0.402	0.424	6.081	9.318	13.486	15.742	17.749
CARR-CJ	0.262	0.320	0.368	0.390	0.409	5.967	9.179	13.069	15.120	16.875
Ratio	**0.991**	**0.986**	**0.976**	**0.970**	**0.964**	**0.981**	**0.985**	**0.969**	**0.961**	**0.951**
DM stat.	−1.561	−2.650***	−5.251***	−6.945***	−10.046***	−2.177**	−1.698*	−6.013***	−7.534***	−10.365***
Model	*Fraction of times a model is the best*									
CARR	0%	0%	0%	0%	0%	20%	20%	0%	0%	0%
CARR-CJ	100%	100%	100%	100%	100%	80%	80%	100%	100%	100%

NOTE: This table computes the RMSE and QLIKE using the following equations:

$$\mathrm{RMSE}(m,h)=\left[T^{-1}\sum_{t=1}^{T}\left(\mathrm{MV}_{t+h}-\mathrm{FV}_{t+h}(m)\right)\right]^{0.5},\quad \mathrm{QLIKE}(m,h)=T^{-1}\sum_{t=1}^{T}\left(\frac{\mathrm{MV}_{t+h}}{\mathrm{FV}_{t+h}(m)}-\ln\left(\frac{\mathrm{MV}_{t+h}}{\mathrm{FV}_{t+h}(m)}\right)-1\right),$$

where MV_t and $\mathrm{FV}_t(m)$ are the measure of volatility and the predictions reported by model m, respectively. All tests are out-of-sample and carried out using expanding window approach for a robustness check. We only report cases with h =1, 5, 22, 44, and 66 days. Smaller RMSE (QLIKE) means lower forecasting error. Bold entries and negative values of the DM test indicate that the CARR-CJ model beats the CARR model. The RMSE and QLIKE reported in this table have been multiplied by 100. The bottom rows report the list of models and the fraction of times a given model is best across the five equity indices for a given horizon. ***, **, and * represent 1%, 5%, and 10% levels of significance, respectively.

In-sample results are reported in Table 10. As expected, all coefficients of leverage are positive and highly significant. A closer look at the magnitudes shows that the leverage effects are higher for the continuous component than for the jump component, which implies a heterogeneous structure of the leverage effect for these two range processes as well. Moreover, by comparing Table 4 and Table 10, the LLF show unambiguously that inclusion of the leverage effect improves the in-sample forecasting performance, except for the HSI index. On the other hand, reduction of Lung–Box Q statistic for the CARRX and CARRX-CJ models in most cases, compared with the CARR and CARR-CJ models, is remarkable. It is clear that a pure CARR or CARR-CJ model is

TABLE 10
IN-SAMPLE ESTIMATION RESULTS OF THE CARRX AND CARRX-CJ MODELS

	$\omega\times10^4$	α	β	γ	Half-life	LLF	Q(12)
Panel A: AORD							
CARRX	2.389(0.000)	0.074(0.000)	0.859(0.000)	0.084(0.000)	28.465	187.219	12.510(0.406)
CARRX-C	2.285(0.000)	0.083(0.000)	0.850(0.000)	0.083(0.000)	27.858	187.225	12.445(0.411)
CARRX-J	0.325(0.000)	0.002(0.729)	0.960(0.000)	0.052(0.000)	58.526		
Panel B: DJI							
CARRX	3.057(0.000)	0.104(0.000)	0.809(0.000)	0.125(0.000)	29.213	174.696	18.997(0.089)
CARRX-C	2.997(0.000)	0.131(0.000)	0.784(0.000)	0.113(0.000)	25.281	174.708	19.179(0.084)
CARRX-J	0.540(0.000)	0.019(0.012)	0.928(0.000)	0.089(0.000)	86.601		
Panel C: HSI							
CARRX	1.997(0.000)	0.088(0.000)	0.880(0.000)	0.033(0.000)	44.801	164.497	15.539(0.213)
CARRX-C	2.013(0.000)	0.095(0.000)	0.872(0.000)	0.033(0.000)	41.572	164.500	13.477(0.335)
CARRX-J	0.393(0.000)	0.022(0.001)	0.954(0.000)	0.026(0.000)	64.780		
Panel D: NK 225							
CARRX	4.247(0.000)	0.142(0.000)	0.786(0.000)	0.079(0.000)	22.126	164.125	29.393(0.003)
CARRX-C	3.835(0.000)	0.147(0.000)	0.783(0.000)	0.077(0.000)	22.511	164.130	31.821(0.001)
CARRX-J	0.575(0.000)	0.029(0.000)	0.938(0.000)	0.039(0.000)	53.173		
Panel E: S&P 500							
CARRX	2.999(0.000)	0.096(0.000)	0.814(0.000)	0.133(0.000)	29.838	174.320	24.092(0.020)
CARRX-C	3.109(0.000)	0.116(0.000)	0.792(0.000)	0.126(0.000)	25.007	174.336	22.997(0.028)
CARRX-J	0.328(0.000)	0.018(0.011)	0.934(0.000)	0.088(0.000)	175.086		

NOTE: This table reports the estimation results of the CARRX and CARRX-CJ models with the leverage effect. The CARRX model $\lambda_t = \omega + \alpha R_{t-1} + \beta\lambda_{t-1} + \gamma I(r_{t-1}<0)R_{t-1}$, where R_t is the range and r_t is the log return. The CARRX-CJ model $\lambda_t^C = \omega^C + \alpha^C CR_{t-1} + \beta^C\lambda_{t-1}^C + \gamma^C I(r_{t-1}<0)CR_{t-1}$ and $\lambda_t^J = \omega^J + \alpha^J JR_{t-1} + \beta^J\lambda_{t-1}^J + \gamma^J I(r_{t-1}<0)JR_{t-1}$, where CR_t and JR_t are the continuous and jump parts of the range, respectively. Both CARR and CARR-CJ models are estimated using the QMLE method. LLF is the log-likelihood function and is multiplied by 10^{-2}. $Q(k)$ is the Ljung–Box Q statistic for autocorrelation test with k lags. The numbers in parentheses are p-values for model coefficients and Q(k) statistic.

insufficient and that exogenous variables are necessary to warrant a model to pass misspecification tests. Also, the estimation results consistently show that the jump component is quite persistent, with a volatility half-life of about 53 to 175 days, while it has a smaller short-run impact on future volatility than the continuous component.[16]

4.4 Further Analysis

Given that the CARR-CJ model is designed to capture the market dynamics of the continuous variation and jumps in volatility, it is unsurprising that it outperforms the standard CARR model. An even more interesting question is whether it can beat the existing jump volatility models. In this paper, we use the most popular HAR-CJ model of Andersen et al. (2007) as the benchmark jump model for forecasting return volatility. The specification of HAR-CJ is defined as follows:

$$RV_{t,t+1} = \beta_0 + \beta_{CD}C_{t\text{-}1,t} + \beta_{CW}C_{t-5,t} + \beta_{CM}C_{t-22,t} + \beta_{JD}J_{t-1,t} + \beta_{JW}J_{t-5,t} + \beta_{JM}J_{t-22,t} + \varepsilon_{t,t+1}^{CJ}, \quad (33)$$

where $RV_{t,t+1}$ is the increment of RV from t to $t+1$, $C_{t\text{-}1,t}$, $C_{t-5,t}$, and $C_{t-22,t}$ are the averages of the lagged daily, weekly, and monthly continuous components, respectively, $J_{t\text{-}1,t}$, $J_{t-5,t}$, and $J_{t-22,t}$ are the averages of the lagged daily, weekly, and monthly jump components, respectively, and $\varepsilon_{t,t+1}^{CJ}$ is an innovation term. The HAR-CJ model separates each of the RV components of the

[16] The persistence parameter is measured by $\alpha + \beta + 0.5\gamma$.

TABLE 11
RMSE AND QLIKE STATISTICS OF THE OUT-OF-SAMPLE FORECASTS ON REALIZED VOLATILITY BY CARRX AND CARRX-CJ: ROLLING WINDOW APPROACH (ROBUSTNESS CHECK)

	RMSE					QLIKE				
	Horizon (days)					Horizon (days)				
	1	**5**	**22**	**44**	**66**	**1**	**5**	**22**	**44**	**66**
Panel A: AORD										
CARRX	0.197	0.220	0.242	0.249	0.256	4.683	5.877	7.369	7.909	8.406
CARRX-CJ	0.196	0.219	0.240	0.246	0.253	4.656	5.841	7.260	7.746	8.215
Ratio	**0.996**	**0.995**	**0.992**	**0.990**	**0.989**	**0.994**	**0.994**	**0.985**	**0.979**	**0.977**
DM stat.	−1.786*	−2.192**	−3.617***	−4.677***	−5.596***	−1.355	−1.140	−3.155***	−4.617***	−5.265***
Panel B: DJI										
CARRX	0.282	0.350	0.403	0.428	0.445	5.767	9.229	13.811	16.076	17.489
CARRX-CJ	0.279	0.344	0.390	0.411	0.425	5.567	8.969	13.082	15.008	16.208
Ratio	**0.988**	**0.981**	**0.968**	**0.962**	**0.955**	**0.965**	**0.972**	**0.947**	**0.934**	**0.927**
DM stat.	−1.444	−3.459***	−5.597***	−7.164***	−9.937***	−3.547***	−2.688***	−5.540***	−7.069***	−8.772**
Panel C: HSI										
CARRX	0.222	0.249	0.274	0.276	0.292	3.639	4.443	5.565	5.959	6.763
CARRX-CJ	0.219	0.246	0.269	0.271	0.286	3.515	4.322	5.411	5.730	6.495
Ratio	**0.984**	**0.986**	**0.984**	**0.980**	**0.978**	**0.966**	**0.973**	**0.972**	**0.962**	**0.960**
DM stat.	−5.933***	−4.132***	−4.502***	−7.444***	−8.749***	−7.681***	−4.852***	−4.796***	−8.153***	−8.960***
Panel D: NK 225										
CARRX	0.312	0.368	0.419	0.433	0.442	5.062	7.607	10.942	12.006	12.735
CARRX-CJ	0.328	0.371	0.419	0.431	0.441	6.087	7.891	10.879	11.839	12.560
Ratio	1.053	1.008	**1.000**	**0.997**	**0.996**	1.202	1.037	**0.994**	**0.986**	**0.986**
DM stat.	5.691***	1.034	−0.015	−0.571	−0.666	6.049***	1.832*	−0.409	−1.136	−1.334
Panel E: S&P 500										
CARRX	0.254	0.328	0.389	0.417	0.442	5.811	9.518	14.444	17.012	18.951
CARRX-CJ	0.250	0.321	0.374	0.398	0.417	5.607	9.254	13.650	15.819	17.448
Ratio	**0.984**	**0.978**	**0.963**	**0.955**	**0.945**	**0.965**	**0.972**	**0.945**	**0.930**	**0.921**
DM stat.	−2.369**	−3.915***	−6.018***	−7.790***	−11.382***	−4.307***	−3.107***	−7.080***	−8.296***	−10.342***
Model	*Fraction of times a model is the best*									
CARRX	20%	20%	0%	0%	0%	20%	20%	0%	0%	0%
CARRX-CJ	80%	80%	100%	100%	100%	80%	80%	100%	100%	100%

NOTE: This table computes the RMSE and QLIKE using the following equations:

$$\mathrm{RMSE}(m,h)=\left[T^{-1}\sum_{t=1}^{T}\left(\mathrm{MV}_{t+h}-\mathrm{FV}_{t+h}(m)\right)\right]^{0.5},\quad \mathrm{QLIKE}(m,h)=T^{-1}\sum_{t=1}^{T}\left(\frac{\mathrm{MV}_{t+h}}{\mathrm{FV}_{t+h}(m)}-\ln\left(\frac{\mathrm{MV}_{t+h}}{\mathrm{FV}_{t+h}(m)}\right)-1\right),$$

where MV_t and $\mathrm{FV}_t(m)$ are the measure of volatility and the predictions reported by model m, respectively. All tests are out-of-sample and carried out using the rolling window approach. We only report cases with h =1, 5, 22, 44, and 66 days. Smaller RMSE (QLIKE) means lower forecasting error. Bold entries and negative values of the DM test indicate that the CARRX-CJ model beats the CARRX model. The RMSE and QLIKE reported in this table have been multiplied by 100. The bottom rows report the list of models and the fraction of times a given model is best across the five equity indices for a given horizon. ***, **, and * represent 1%, 5%, and 10% levels of significance, respectively.

HAR framework of Corsi (2009) into its continuous and discontinuous (jump) parts. The empirical results in Corsi et al. (2010) suggested that the separation strategy introduced by this model significantly improved the out-of-sample forecasting.

Table 12 presents the summary statistics for the one-step-ahead out-of-sample forecast evaluations.[17] It is clear that the CARR-CJ model exhibits superior forecasting performance for five equity markets, since it reports lower RMSE and lower QLIKE. The DM statistics are negative

[17] Note, however, that we are not able to produce multi-step forecasts. To do so, we need to feed the continuous and jump forecasts from each successive step back into the HAR-CJ model to generate the next step, but, in fact, that strictly could not be achieved unless we set up two different volatility models to capture their dynamic movements.

TABLE 12
RMSE AND QLIKE STATISTICS OF THE OUT-OF-SAMPLE FORECASTS ON REALIZED VOLATILITY BY THE HAR-CJ AND CARR-CJ MODELS

	Rolling window		Expanding window	
	RMSE	**QLIKE**	**RMSE**	**QLIKE**
Panel A: AORD				
HAR-CJ	0.208	5.184	0.208	5.175
CARR-CJ	0.200	4.815	0.200	4.848
Ratio	**0.959**	**0.929**	**0.961**	**0.937**
DM stat.	−3.312***	−3.559***	−2.873***	−2.892***
Panel B: DJI				
HAR-CJ	0.317	8.284	0.317	8.284
CARR-CJ	0.290	5.960	0.292	5.990
Ratio	**0.914**	**0.720**	**0.919**	**0.723**
DM stat.	−5.557***	−9.432***	−4.664***	−8.772***
Panel C: HSI				
HAR-CJ	0.229	3.798	0.229	3.798
CARR-CJ	0.220	3.529	0.222	3.588
Ratio	**0.959**	**0.929**	**0.971**	**0.945**
DM stat.	−1.672*	−2.729***	−1.263	−2.161**
Panel D: NK 225				
HAR-CJ	0.336	5.997	0.335	6.089
CARR-CJ	0.315	5.133	0.316	5.159
Ratio	**0.935**	**0.856**	**0.943**	**0.847**
DM stat.	−2.974***	−5.539***	−2.878***	−5.678***
Panel E: S&P 500				
HAR-CJ	0.286	8.273	0.283	7.757
CARR-CJ	0.261	5.991	0.262	5.967
Ratio	**0.912**	**0.724**	**0.925**	**0.769**
DM stat.	−4.095***	−3.912***	−3.201***	−6.047***

NOTE: This table computes the RMSE and QLIKE using the following equations:

$$\mathrm{RMSE}(m,h)=\left[T^{-1}\sum_{t=1}^{T}\left(\mathrm{MV}_{t+h}-\mathrm{FV}_{t+h}(m)\right)\right]^{0.5},\quad \mathrm{QLIKE}(m,h)=T^{-1}\sum_{t=1}^{T}\left(\frac{\mathrm{MV}_{t+h}}{\mathrm{FV}_{t+h}(m)}-\ln\left(\frac{\mathrm{MV}_{t+h}}{\mathrm{FV}_{t+h}(m)}\right)-1\right),$$

where MV_t and $\mathrm{FV}_t(m)$ are the measure of volatility and the predictions reported by model m, respectively. All tests are one-step-ahead out-of-sample and carried out using the rolling window and expanding window approaches. Smaller RMSE (QLIKE) means lower forecasting error. Bold entries and negative values of the DM test indicate that the CARR-CJ model beats the HAR-CJ model. The RMSE and QLIKE reported in this table have been multiplied by 100. ***, **, and * represent 1%, 5%, and 10% levels of significance, respectively.

and significant in most cases, which means that the dominance of the CARR-CJ model over the HAR-CJ model is statistically significant. It is found that the range-based model with a non-linear structure has better forecasting accuracy than the HAR realized volatility linear model. Therefore, the predictive ability of the extension model in this paper is very encouraging.

Turning to the out-of-sample evidence, Table 11 reports the out-of-sample forecasting performance for realized volatility, carried out by the rolling window method. The superiority of the CARRX-CJ model with the leverage effect is also confirmed in most cases, especially at longer horizons. The above robustness tests show that our findings are quite robust and largely benefit from the separation of the price range into its continuous and discontinuous (jump) components.

5. CONCLUSIONS

In this paper, we construct a novel range-based model with jumps that extends the CARR model by decomposing the price range into its continuous and jump components. Based on the framework of the CARR model, we are able to directly investigate the dynamics of the volatility shocks in nature, i.e., the short-run impact and volatility persistence. To the best of our knowledge, the present study is the first to incorporate jumps in a low-frequency data based price range modeling and forecasting under the CARR specification instead of the HAR-type models. Our empirical results, obtained on the international equity markets, show that the jump component has longer volatility half-life and smaller short-run impact on future volatility compared to the continuous component, an indication that the dynamics for the two parts of the range differ greatly. On the other hand, the CARR-CJ model we propose provides a superior in-sample fit and out-of-sample forecasting performance to the CARR benchmark as well as the HAR-CJ model of realized volatility, especially at longer forecast horizons. Moreover, our study's results are quite robust to employ other volatility measures and forecast evaluation methods, as well as include well-known exogenous variables, such as the leverage effect, into the CARR-CJ model.

These findings contribute to the extant literature in several ways. First, the existing studies exploring the role of jumps in price are mostly grounded upon realized return-based volatility and HAR framework. Hence, our paper attempts to model and forecast price range with jumps in the framework of the CARR model, which should enrich the related research on volatility jumps. Second, our study demonstrates that by slightly modifying the CARR model to allow and control for jumps, the resulting CARR-CJ model outperforms the most popular HAR-CJ model of realized volatility, owing to our model's greater flexibility in capturing the dynamic evolution of volatilities, such as time-varying volatility and volatility clustering. Third, as pointed out by Chou (2005), our model is very simple to implement, as the estimation of the model parameters can be performed through estimating a well-known GARCH model. Finally, the aggregate daily realized measures data used to split a range into two parts is free and publicly available; thus, access to the high-frequency intraday data from which these realized measures were not required. We think that, for all the aforementioned contributions, the extension model may be effectively used for risk management and asset pricing.

LITERATURE CITED

Aït-Sahalia, Y. (2002), "Telling from Discrete Data Whether the Underlying Continuous-Time Model Is a Diffusion," *Journal of Finance*, **57**(5), 2075–2112.

Aït-Sahalia, Y. (2004), "Disentangling Diffusion from Jumps," *Journal of Financial Economics*, **74**(3), 487–528.

Aït-Sahalia, Y. and J. Jacod (2012), "Analyzing the Spectrum of Asset Returns: Jump and Volatility Components in High Frequency Data," *Journal of Economic Literature*, **50**(4), 1007–1050.

Ahoniemi, K. and M. Lanne (2013), "Overnight Stock Returns and Realized Volatility," *International Journal of Forecasting*, **29**(4), 592–604.

Andersen, T. G., L. Benzoni, and J. Lund (2002), "An Empirical Investigation of Continuous-Time Equity Return Models," *Journal of Finance*, **57**(3), 1239–1284.

Andersen, T. G., T. Bollerslev, and F. X. Diebold (2007), "Roughing It Up: Including Jump Components in the Measurement, Modeling and Forecasting of Return Volatility," *The Review of Economics and Statistics*, **89**(4), 701–720.

Andersen, T. G., T. Bollerslev, F. X. Diebold, and P. Labys (2000), "Great Realizations," *Risk*, **13**(3), 105–108.

Andersen, T. G., D. Dobrev, and E. Schaumburg (2009), *Jump-Robust Volatility Estimation Using Nearest Neighbor Truncation*, NBER Working Papers 15533, Cambridge, MA: National Bureau of Economic Research, Inc.

Barndorff-Nielsen, O. E. and N. Shephard (2004), "Power and Bipower Variation with Stochastic Volatility and Jumps," *Journal of Financial Econometrics*, **2**(1), 1–37.

Barndorff-Nielsen, O. E. and N. Shephard (2006), "Econometrics of Testing for Jumps in Financial Economics Using Bipower Variation," *Journal of Financial Econometrics*, **4**(1), 1–30.

Black, Fischer (1976), "Studies of Stock, Price Volatility Changes," *Proceedings of the 1976 Meetings of the Business and Economics Statistics Section.* American Statistical Association.

Bollerslev T, R. F. Engle, and D. Nelson (1994), "ARCH Models," *In Handbook of Econometrics*, Vol. IV, Engle R. F. and D. L. McFadden (Eds). Elsevier Science B. V.: Amsterdam; 2961–3038.

Brandt, M. W. and C. S. Jones (2006), "Volatility Forecasting with Range-Based EGARCH Models," *Journal of Business & Economic Statistics*, **24**(4), 470–486.

Buncic, D. and K. I. Gisler (2017), "The Role of Jumps and Leverage in Forecasting Volatility in International Equity Markets," *Journal of International Money and Finance*, **79**(C), 1-19.

Caporin M., E. Rossi, and P. S. D. Magistris (2015), "Volatility Jumps and Their Economic Determinants," *Journal of Financial Econometrics*, **14**(1), 29–80.

Chen, W. P., T. Choudhry, and C. C. Wu (2013), "The Extreme Value in Crude Oil and US Dollar Markets," *Journal of International Money and Finance*, **36**(C), 191–210.

Chong, Y. Y. and D. F. Hendry (1986), "Econometric Evaluation of Linear Macro-Economic Models," *Review of Economic Studies*, **53**(4), 671–690.

Chou, R. Y. (2005), "Forecasting Financial Volatilities with Extreme Values: The Conditional Autoregressive Range (CARR) model," *Journal of Money, Credit and Banking*, **37**(3), 561–582.

Chou, R. Y., H. C. Chou, and N. Liu (2015), Range Volatility: A Review of Models and Empirical Studies, In C. F. Lee and J. C. Lee (Eds.), *Handbook of Financial Econometrics and Statistics*, Berlin, Germany: Springer, 2029–2050.

Chou, R. Y. and N. Liu (2010), "The Economic Value of Volatility Timing Using a Range-Based Volatility Model," *Journal of Economic Dynamics and Control*, **34**(11), 2288–2301.

Christensen, K., R. Oomen, and M. Podolskij (2010), "Realised Quantile-Based Estimation of the Integrated Variance," *Journal of Econometrics*, **159**(1), 74–98.

Christensen, K. and M. Podolskij (2006), "Range-Based Estimation of Quadratic Variation (no.

2006, 37)," Technical Report/Universität Dortmund (SFB 475 Komplexitätsreduktion in Multivariaten Datenstrukturen).

Christensen, K. and M. Podolskij (2007), "Realized Range-Based Estimation of Integrated Variance," *Journal of Econometrics*, **141**(2), 323–349.

Corsi, F. (2009), "A Simple Approximate Long-Memory Model of Realized Volatility," *Journal of Financial Econometrics*, **7**(2), 174–196.

Corsi, F., D. Pirino, and R. Renò (2010), "Threshold Bipower Variation and the Impact of Jumps on Volatility Forecasting," *Journal of Econometrics*, **159**(2), 276–288.

Corsi, F. and R. Renò (2012), "Discrete-Time Volatility Forecasting with Persistent Leverage Effect and the Link with Continuous-Time Volatility Modeling," *Journal of Business & Economic Statistics*, **30**(3), 368–380.

Degiannakis, S. and A. Livada (2013), "Realized Volatility or Price Range: Evidence from a Discrete Simulation of the Continuous Time Diffusion Process," *Economic Modelling*, **30**(C), 212–216.

Diebold, F. X. and R. S. Mariano (1995), "Comparing Predictive Accuracy," *Journal of Business & Economic Statistics*, **13**(3), 253–263.

Engle, R. F. (2002), "New Frontiers for ARCH Models," *Journal of Applied Econometrics*, **17**(5), 425–446.

Engle, R. F. and A. J. Patton (2001), "What Good Is a Volatility Model?" *Quantitative Finance*, **1**(2), 237–245.

Engle, R. F. and J. R. Russell (1998), "Autoregressive Conditional Duration: A New Model for Irregularly Spaced Transaction Data," *Econometrica*, **66**(5), 1127–1162.

Eraker, B., M. Johannes, and N. Polson (2003), "The Impact of Jumps in Volatility and Returns," *The Journal of Finance*, **58**(3), 1269–1300.

Garman, M. B. and M. J. Klass (1980), "On the Estimation of Security Price Volatilities from Historical Data," *Journal of Business*, **53**(1), 67–78.

Hansen, P. R. and A. Lunde (2006), "Consistent Ranking of Volatility Models," *Journal of Econometrics*, **131**(1-2), 97–121.

Heber, Gerd, Asger Lunde, Neil Shephard and Kevin Sheppard (2009), "Oxford-Man Institute's Realized Library," Oxford-Man Institute, University of Oxford.

Huang, X. and G. Tauchen (2005), "The Relative Contribution of Jumps to Total Price Variance," *Journal of Financial Econometrics*, **3**(4), 456–499.

Jiang, G. and R. Oomen (2008), "Testing for Jumps When Asset Prices Are Observed with Noise–A "Swap Variance" Approach," *Journal of Econometrics*, **144**(2), 352–370.

Lee, S. S. and P. A. Mykland (2008), "Jumps in Financial Markets: A New Nonparametric Test and Jump Dynamics," *Review of Financial Studies*, **21**(6), 2535–2563.

Ma, F., Y. Zhang, D. Huang, and X. Lai (2018), "Forecasting Oil Futures Price Volatility: New Evidence from Realized Range-Based Volatility," *Energy Economics*, **75**, 400–409.

Mancini, C. (2009), "Non-Parametric Threshold Estimation for Models with Stochastic Diffusion Coefficient and Jumps," *Scandinavian Journal of Statistics*, **36**(2), 270–296.

Merton, R. C. (1976), "Option Pricing When Underlying Stock Returns Are Discontinuous," *Journal of Financial Economics*, **3**(1-2), 125–144.

Mincer, J. A. and V. Zarnowitz (1969), "The Evaluation of Economic Forecasts," in *Economic Forecasts and Expectations: Analysis of Forecasting Behavior and Performance*, Ed., J. A. Mincer, 3-46, New York: Columbia University Press.

Molnár, P. (2016), "High–Low Range in GARCH Models of Stock Return Volatility," *Applied Economics*, **48**(51), 4977–4991.

Nelson, D. (1991), "Conditional Heteroskedasticity in Asset Returns: A New Approach," *Econometrica*, **59**(2), 347–370.

Parkinson, M. (1980), "The Extreme Value Method for Estimating the Variance of the Rate of Return," *The Journal of Business*, **53**(1), 61–65.

Patton, A. J. (2011), "Volatility Forecast Comparison Using Imperfect Volatility Proxies," *Journal of Econometrics*, **160**(1), 246–256.

Podolskij, M. and D. Ziggel (2010), "New Tests for Jumps in Semimartingale Models," *Statistical Inference for Stochastic Processes*, **13**(1), 15–41.

Welch, I. and A. Goyal (2008), "A Comprehensive Look at the Empirical Performance of Equity Premium Prediction," *Review of Financial Studies*, **21**(4), 1455–1508.

Xie, H. (2019), "Financial Volatility Modeling: The Feedback Asymmetric Conditional Autoregressive Range Model," *Journal of Forecasting*, **38**(1), 11–28.